TRIBHUVAN UNIVERSITY

INSTITUTE OF ENGINEERING

PULCHOWK CAMPUS

Thesis no: M-18-MSMSDE-2017/2019

Optimization of Closure Law of Guide Vanes of Francis Turbine : A Case Study of a Typical Operational Hydropower Project of Nepal

By

Saroj Chalise

A THESIS REPORT

SUBMITTED TO THE DEPARTMENT OF MECHANICAL ENGINEERING

IN PARTIAL FULFILLMENT OF THE REQUIREMENTS FOR THE DEGREE OF MASTER OF SCIENCE IN MECHANICAL SYSTEM DESIGN AND ENGINEERING

DEPARTMENT OF MECHANICAL ENGINEERING

LALITPUR, NEPAL

NOVEMBER, 2019

COPYRIGHT

TRIBHUVAN UNIVERSITY

INSTITUTE OF ENGINEERING

PULCHOWK CAMPUS

DEPARTMENT OF MECHANICAL ENGINEERING

The undersigned certify that they have read, and recommended to the Institute of Engineering for acceptance, a thesis entitled "Optimization of Closure Law of Guide Vanes : A Case Study of Typical Operational Hydropower Project of Nepal" submitted by Saroj Chalise in partial fulfillment of the requirements for the degree of Master of Science in Mechanical System Design and Engineering.

Supervisor, Laxman Poudel, Ph.D.

Professor

Department of Mechanical engineering

External Examiner, Bhola Thapa, Ph.D.

Professor

Kathmandu University

Committee Chairperson, Nawraj Bhattarai, Ph.D.

Head of Department

Department of Mechanical Engineering,

Date:

ABSTRACT

This thesis addresses the optimization of closure law of guide vanes of Francis turbine in an operational hydropower plant. Sanima Mai Hydropower Project (22 MW), located at Ilam district of Nepal has been taken as primary reference. A mathematical model has been developed using the Bentley hammer software to model the hydraulic transient parameters during the full load rejection. The mathematical model is validated by comparing the results of the model with the data of the load rejection test which were carried out during commissioning phase of the project. The value of rise of maximum pressure and maximum speed as obtained from the model is compared with data of load rejection test for various closure time. The comparison of these result shows that the maximum discrepancy between numerical and experimental data is 3.2 %, hence concluding the reliability of the developed mathematical model.

Various combinations of single-phase linear and three-phase close-delay-close (CDC) closure patterns have been applied to the validated model to study the effect of the closure pattern. The value of maximum hydrodynamic pressure and the maximum rotational speed of turbine are calculated for all the cases of guide vane closure. To quantify the effectiveness of a closure pattern to harmonize the rise of hydrodynamic pressure and the rotational speed of turbine, a non-linear objective function has been proposed and based on the extent of the minimization of the defined objective function, different closure laws are compared. For a single-phase closure law, the maximum pressure decreases and the maximum speed increases on increasing the closure time and vice-versa. The optimum closure law for single phase linear closure pattern is obtained at closure time of seven seconds which keeps the maximum pressure and maximum speed at 1542 KPA and 755 RPM respectively .The corresponding value of objective function is 6.4.

For a three-phase CDC pattern, maximum speed increases on increasing any of the four parameters; t_1, t_2, t_3 and s, provided that the remaining three variables remains unchanged. However, there are no any clear trends observed for the maximum pressure. Nevertheless, it has been concluded that the value of objective function is better

controlled when the speed of first closure is faster than the speed of second closure. The optimum closure law for a three phase CDC pattern is obtained at t_1= 4 second, t_2= 5 second, t_3 = 9 second and s= 0.35 which keeps the maximum pressure and maximum speed at 1507 KPA and 754 RPM respectively. The corresponding objective function is 5.6.

The optimum closure law obtained in both the pattern ensures the target hydraulic transient parameters within the defined range. Moreover, the comparison of the value of objective function for single phase and three phase CDC linear closure pattern concludes that the three-phase CDC pattern ensures better regulation than the single phase closure pattern.

Keywords: Closure law, Guide vane, Optimization, Hydraulic transients

ACKNOWLEDGEMENT

I would like to extend my sincere gratitude towards my thesis supervisor Prof. Dr. Laxman Poudel for his professional guidance, enthusiastic encouragement and useful critiques throughout my thesis work duration. This thesis work would not have been possible without his assistance and encouragement.

I am indebted to Sanima Mai Hydropower Limited, for providing me the necessary drawings and data to carry out analysis for this thesis work.

At last but not the least, I would like to express my appreciation to all my respected teachers and colleagues who have contributed in any way to accomplish this work.

TABLE OF CONTENTS

LIST OF TABLES

LIST OF FIGURES

LIST OF ACRONYMS AND ABBREVATIONS

CCC	:	Close-close-close
CDC	:	Close-delay-close
CFL	:	Courant Friedrick-Lewy
CGIHTM	:	Characteristics Graph based Iterative Hydro turbine model
CLGV	:	Closure Law of guide Vane
CRC	:	Close-reopen-close
GA	:	Genetic Algorithm
KPa	:	Kilopascal
KV	:	Kilovolt
KVA	:	Kilovolt Ampere
MOC	:	Methods of Characteristics
MPa	:	Mega Pascal
MW	:	Megawatt
ODE	:	Ordinary Differential equation
PDE	:	Partial Differential Equation
RPM	:	Revolution per minute

CHAPTER ONE: INTRODUCTION

1.1. Background

Nepal is rich in hydropower with 83,000 MW of theoretical and 42,133 MW of technically/financially viable potential. The total capacity based on run-of-river basis at Q40 (flow exceedance) and 80 % total efficiency is 53,8334 MW; with annual energy of 346,538 GWh (Jha 2010). Being a country having good potential of hydropower, the research on safe and reliable operation of hydropower is equally important. Normal functioning of the hydropower under steady-state condition is safe. However, there are several factors that interrupt the steady-state operation, which includes load rejection or acceptance by the electricity grid, faults at the equipment of generating station and so on. Recalling to the past accidents on hydropower, most of them were due to undesired values of hydraulic transient parameters (Pressure, head and speed) during the unsteady state (Adamkowski, 2001). Hence, the design of the equipment at the generating station should be carefully done so that the hydraulic transient parameters during the unsteady state can be ensured within safe limit.

Various strategies can be implemented to an operational hydropower project to ensure the safe operation from the perspective of controlled values of pressure and rotational speed. This includes, installation of pressure relief valves, installation of rupture disc , modification of the water conveyance network, modification of generator flywheel to increase the moment of inertia (GD^2) of the rotating components and so on (Bergant et al., 2014 ; Shariff et al., 2014). However, compared to these options, variation of the closure law of guide vane (CLGV) is the most economical option, since the closure law can be modified from the governor without installation and modification of any new equipment (Sheng et al., 2014; Cui et al., 2014).

The optimization of the closure law is namely to make controlling parameters, maximum water hammer pressure rise and rotating speed rise of the units, satisfy the requirements of guaranteed regulation calculation through changing the different parameters of the closure law. This thesis works mainly discusses the single-stage and three-phase closure law and its optimization. The popular characteristics method is

introduced to establish the mathematic model of the hydraulic transient process and its correctness is validated by comparing the results of the calculation and corresponding field test. Consequently, the model is applied for optimization of CLGV.

1.2. Problem Statement

The rotating speed rise and maximum water hammer pressure are closely related to the closure law of the wicket gate. The rotational speed of the turbine-generator assembly rises soon after the load rejection; hence, the guide vanes of a Francis turbine should be closed fast enough to prevent the rotating components from excessive rotational speed. However, the sudden closure of the guide vanes creates the hydraulic transient condition in the waterway network located upstream and downstream of the turbine (Wiley and Streeter, 1993). During transient condition, water pressure fluctuates from maximum to minimum value in the entire water conduit, which if not designed carefully, can pose the risk of either bursting due to extremely high pressure or the cavitation due to extremely low pressure in the different sections of the pipe (Chaudhry, 2014)

Therefore, there is no doubt that a guaranteed regulation calculation is needed to propose the rational closure law to limit both the maximum water pressure and rotating speed rise within the allowable range. The limitation of water hammer pressure and rotating speed rise is a pair of contradictions, and the focus of the contradiction is the closure law of guide vane (CLGV). Hence, optimization of closure law is most important in the design phase of hydropower. Moreover, in an operational hydropower plant, changing of the CLGV is the most economical and preferred option to solve the problem of hydraulic transient, since it does not requires any modification or addition of the equipment.

1.3. Research Objective

1.3.1. Main Objective

To optimize the closure law of wicket gate of turbine for safe operation of a specific hydropower project

1.3.2. Specific Objectives

a) To develop a mathematical model for solving transient parameters during instant load rejection.

b) To validate the mathematical by comparing results of numerical simulation with the experimental data.

c) To use the validated model to find the parameters of optimum closure law.

1.4. Scope of the work

The optimum closure pattern of guide vane of Francis turbine for a particular project can be found out, thus ensuring safe operation of the project. The achievement of this study can be used by the designer as a reference for similar projects.

1.5. Limitations of the study

The thesis works have following limitations:

a) Control for negative minimum pressure has not been considered for optimization problem.

b) Only linear closure laws of guide vanes have been considered. Curved closure patterns have not been considered in the study.

CHAPTER TWO: LITERATURE REVIEW

2.1 Hydraulic Transient

In any water conveyance system, the demand of the flow fluctuates which is adjusted by the valves or gates located in the waterway path. In a hydropower plant also, the flow demand fluctuates because of load acceptance or rejection by the electrical system. The fluctuation of the flow demand is adjusted by the wicket gates in the Francis turbine. The closure of the wicket gate located downstream of the penstock pipe creates unsteady-flow conditions in the penstock pipes for a certain transient time. During the transient condition, the pressure fluctuates from the maximum to minimum value at different section of the penstock pipe and the pressure wave travels too and forth along the length of the penstock pipe. The water pressure fluctuates temporally from the maximum to minimum values in the entire section of penstock pipe, which if not designed properly can pose the risk of either bursting due to extremely high pressure or the cavitation due to extremely low pressure (Wiley and Streeter, 1993).

2.2 Mathematical modeling of hydraulic transient

2.2.1 Transient in water conduit

There has been various research works on mathematical modeling of hydraulic transient in water conveyance system of hydropower plant. Because of longer length of the penstock pipe, one-dimensional model are computationally cost-effective than the two-dimensional model. Hence 1-D model are preferred over the 2-D model. The continuity and momentum equation during transient condition in a pressurized conduit can be expressed in one-dimension form as equation 2.1 and equation 2.2 (Chaudhry and Hussaini, 1985)

$$\frac{\partial V}{\partial t}+\frac{1}{\rho}\frac{\partial P}{\partial x}+\frac{f\,V|V|}{2D}=0. \qquad \text{Equation 2.1}$$

$$\frac{\partial P}{\partial t}+\rho c^2\frac{\partial V}{\partial x}=0 \qquad \text{Equation 2.2}$$

Equation 2.1 and 2.2 represents a pair of quasi-static hyperbolic partial differential equations. Although the general solution is not possible to these equations, these

equations can be transferred to ordinary differential equations using Methods of Characteristics and then integrated within limits to obtain the solution at defined co-ordinate of space and time. Using the MOC technique, the value of pressure and velocity at i^{th} node and j^{th} time step can be calculated using algebraic equation 2.3 and equation 2.4 (Carlsson, 2016).

$$P_{i,j} = \frac{1}{2}(P_{i-1,j-1} + P_{i+1,j-1}) + \frac{\rho c}{2}(V_{i-1,j-1} - V_{i+1,j-1}) \\ \frac{\rho c}{2}\left(\frac{fc}{2D}\Delta x\left|V_{i-1,j-1}\right| + \frac{fc}{2D}\Delta x V_{i-1,j-1}\left|V_{i+1,j-1}\right|\right)$$

Equation 2.3

$$V_{i,j} = \frac{1}{2}\frac{1}{\rho c}(P_{i-1,j-1} - P_{i+1,j-1}) + \frac{1}{2}(V_{i-1,j-1} + V_{i+1,j-1}) \\ + \frac{1}{2}\left(\frac{fc}{2D}\Delta x V_{i+1,j-1}\left|V_{i+1,j-1}\right| \quad \frac{fc}{2D}\Delta x V_{i-1,j-1}\left|V_{i-1,j-1}\right|\right)$$

Equation 2.4

The accuracy and the stability of the numerical solution using equation 3 and equation 4 depends upon the selection of the friction factor f, wave speed c, time step Δt , and the grid spacing Δx. The following section of thesis summarizes the previous studies which guides on selection of these factors.

a) **Friction factor**

For the computation of friction factor f, there are three popular models; steady friction model , quassi-static friction model and unsteady friction model. The steady friction model assumes constant value of darcy weisbach friction factor during the transient phase. The main demerits associated with the steady frction model is it does not produce sufficient damping of pressure comparison to the measured data (Bergant et al., 2001).

In the quassy steady friction approach (Fok, 1987), the Darcy-Weisbach cofficient at any point depends on the state of the system at the previous time step. For the starting value of the friction coefficient, the relative roughness of each pipe is estimated by means of the Swamee and Jain (1976) approximation of the Moody diagram. For

subsequent time steps, the Reynolds number is computed at each point on the basis of the previous iteration's velocity and then an updated friction coefficient is ascertained.

In unsteady friction factor model, the friction factor from quassi-static model is multiplied by an amplification factor. Numerous contributions has been proposed for unsteady friction one-dimensional 1D models. These unsteady friction models calculated the friction factor based on instantaneous value of acceleration (Bergant et al., 2001 ; Ramos et. al., 2004). Pezzinga et al.(2009) concluded that most of the unsteady friction model based on local instantaneous acceleration can predict only the value of extreme oscilation of head , not the shape. They proposed the unsteady friction model based on local balance of friction force which overcomed the problems of previous models based on instantneous acceleration.

b) **Wave Speed**

The pressure wave speed depends upon property of the pipe and the fluid. For the pipe having thickness e, Diameter D, support factor Ψ and Young's modulus Ev, the water hameer wave speed magnitude in one dimensional flow is expressed in the equation 2.5 (Watters, 1984).

$$c = \sqrt{\frac{E_V}{\rho(1+\frac{DE_v}{eE}\Psi)}} \quad . \qquad \text{Equation 2.5}$$

Where E and ρ are the bulk modulus and density of the fluid. The value of Ψ for pipe anchored against axial movement and having longitudinal expansion joint is expressed in equation 2.6 (Watters, 1984).

$$\Psi = \frac{1}{1+\frac{e}{D}}.(1+2\frac{e}{D}(1+\upsilon).(1+\frac{2e}{D})) \qquad \text{Equation 2.6}$$

c) **Time step and grid spacing**

The selection of time step Δt and grid spacing Δx depends upon the Courant-Friedrich-Lewy (CFL) number, Co, which is defined as the ratio of the actual wave speed and the numerical wave speed .

$$Co = \frac{c\Delta t}{\Delta x} \qquad \text{Equation 2.7}$$

As pointed in many textbooks, CFL number should be less than one to ensure solution remains within the computational domain (Wiley and streeter, 1993; Chaudhry, 2014). However, Urbanowicz (2017) presented the computational compliance criteria (CCC) where he studied the effect of CFL number on the accuracy of the solution for a pipeline having constant wave speed across the length. Comparing to the experimental data, he showed that the application of CFL number less than one only detoriated modelling errors.Hence, the Courant number should be exactly equal to one for accurate modelling. However, for the multiple pipeline system with pipeline with variable wave speed , it is difficult to satisfy CFL condition for every pipe section. Wave speed or pipe-length adjustments and/or interpolations have to be carefully applied to ensure reasonable results (Carlsson, 2016).

2.2.2 Transient in water turbine

For modelling of the transients in francis turbine, characteristics graph-based iterative hydroturbine model (CGIHM) is widely used to predict the rotational speed of runner at any instant of time (Zhang et al., 2015). The following section illustrates the theory of CGIHM model.

The rise of the rotational speed of turbine during the load rejection is governed by the equation 2.8 (Shengh et al., 2013).

$$I\frac{d\omega}{dt} = T_h - T_g \qquad \text{Equation 2.8}$$

Where,

I = Polar moment of inertia of the rotating parts in turbine-generator combination

ω = Angular speed the turbine

T_h = Torque from the water that is spinning the turbine

T_g = Torque from the generator that the turbine is connected to

Re-arranging the equation 2.8 in terms of power of turbine and generator, the governing equation converts to equation 2.9 (Chaudhry, 2014).

$$P_{tur} - \frac{P_{gen}}{\eta_{gen}} = (\frac{2\pi}{60})^2 I N \frac{dN}{dT} \qquad \text{Equation 2.9}$$

Where, P_{tur}= power of turbine, P_{gen}= power of generator, N is the rotational speed of the turbine-generator assembly in RPM. Integrating equation 8 with respect to time the value of speed can be calculated using equation 2.10 (Chaudhry, 2014).

$$N_p = \{N_1^2 + \frac{\Delta t}{I}[0.5(P_{tur1} + P_{turP}) - \frac{P_{genf}}{\eta_{gen}}]\}^{0.5} \qquad \text{Equation 2.10}$$

In which Δt represent the time step and the subscript 1 and P represent the value at the start and end of the time step. The value of P_{tur} is obtained from the turbine characteristics curve . With the known values of I, N_1, P_{genf} and Δt, the speed at any instant of time can be predicted.

2.3 Sensitivity of hydraulic transient parameter

The hydraulic transient parameters; hydrodynamic pressure, rotational speed of the turbine,flow velocity and discharge is highly sensitive on the properties of the penstock pipe, surge protection devices, turbine and the generator. The accurate prediction of the transient parameters requires a researcher to know how much the transient parameters are sensitive to a particular property so as to avoid computational errors because of incorrect assumptions. Various research has been done to study the effect of alteration of these properties on the transient parameters. Bonath et al. (2009) carried out the transient analysis in a hydropower project with the differential surge tank. They studied the variation of transient parameter by varying dimensions of the orifice, the riser, and the main tank, the interdependency are observed, reported and the optimum dimensions are determined. Iliev et al. (2015) did sensitivity of the transient analysis for emergency shutdown scenario of two unit (simultaneously) of a hydropower project by varying various modeling parameters. Pipeline friction factor, Wave speed, Surge tank throttling

coefficient, turbine guide vane closing law and generator inertia were taken as the parameter for sensitivity analysis. The result demonstrated that these parameters are very sensitive and hence they should be accurately modeled during transient analysis. Rezghi et al. (2015) did numerical investigation for sensitivity analysis of hydraulic transient for two parallel pump-turbine units operating at runaway. The results show that the moment of inertia has considerable effect on the maximum torque at unstable condition of runaway. Also, more moment of inertia can well postpone the peak of pressure and rotational speed. By using different values for acoustic wave velocity, output conditions don't show any clear trend.

2.4 Protection of hydraulic transient

Hydraulic transient conditions are very critical from the perspective of safety. Many past research works have focused on implementation of the various strategies to ensure the safety and minimize the negative effect of hydraulic transients. Bergant et al**.** (2012) studied the behavior of air valve on large-scale pipeline apparatus. Dynamic flow test were performed for float type air valve and the events like system startup, pump trip and pump rupture were simulated. Triki et al. (2017) proposed the addition of branched polymeric short penstock at the transient sensitive region. He did a numerical simulation of such strategy for the existing penstock pipe of a hydropower project. The result showed that such a strategy can significantly mitigate the pressure increase and decrease induced by water hammer. Riasi et al. (2017) did analysis of transient response of a hydropower project with presence of surge tank and surge relief valve. The result substantiated that surge relief valve can be used instead of expensive surge tank to relieve transient pressure. Wan et al. (2018**)** proposed an intelligent self-controlled surge tank where the discharge capacity of the connector is appropriately controlled according to the different conditions. Through the help of numerical analysis, it was proved that such intelligent self-controlled surge tank has advantages in pressure control and applicability compared to normal surge tanks.

2.5 Closure law of guide vanes

Closure law of guide vanes (CLGV) is an operating pattern of guide vane which defines the opening of guide vane at any instant of time. The movement of the guide vanes is controlled by the governor, which is executed as the designed CLGV. The CLGV is

often designed as linear functions, with a one or two-phase line, as shown in Fig 2.1 (Zhao et al., 2010 ; Shengh et al., 2013). Apart from these popular CLGVs, the three-phase closure law has been studied in little previous research (Lai et al., 2019). The three-phase CLGV has three basic sub-types, as depicted in figure 2.2. These can be classified by the tendency of the second phase as the "close-reopen-close" (CRC), "close-delay-close" (CDC), and "close-close-close" (CCC) manners. In the CLGV with "CRC", the amplitude of the second phase is negative and it can reduce more water hammer pressure than the other two CLGVs (Zeng et al., 2015).

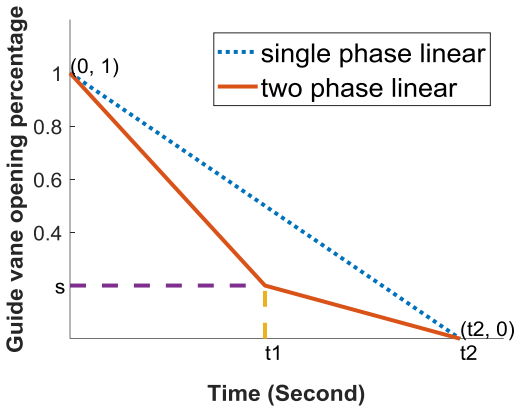

Figure 2. 1 Single and two-phase linear closure law of guide vanes

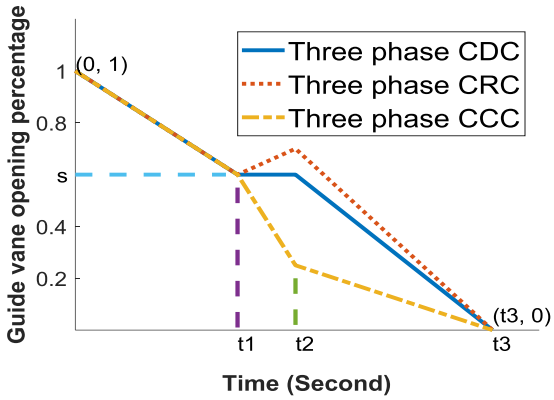

Figure 2. 2 Various types of three-phase linear closure law of guide vanes

Source : Lai et al., (2019)

There has been little research on the study of the impact of the closure law of guide vanes on the transient parameters. Zhao et al. (2010) studied closing law of guide vanes in high, middle and low head, and establishes the multi-objective optimal model of the closing law. They concluded that closure pattern of "slow after fast" is more suitable than the closure pattern of "fast after slow" for low and medium head hydropower plant. Sheng et al. (2013) developed a mathematical model of transient process is established by introducing the method of characteristic, whose correctness is validated by the field test. Then the model is applied to a specific hydropower station that only can employ closure law optimization to coordinate the contradiction between pressure and speed rise, for two-stage closure optimization. Li et. al (2013) presented a wicket gate step-by-step closure control law, where two guide vanes will be closed asynchronously to reduce the increase in pressure and improve the transient quality of a water turbine. Compared with the calculated data in the routine closure law, the control

law obviously improved the dynamic qualities of the transient in load rejection and decreased the rising hydraulic pressure from the water diversion system of the plant. The proposed control law can replace the role of a surge tank under certain conditions. Cui et al. (2014) developed a new non-linear evaluating function and used genetic algorithm to optimize the wicket gate closure law. The numerical calculation results show that the new non-linear evaluating function is of great advantages compared to traditional evaluating function in distribution of safety margin of each optimization goal. Optimized WG closing law by multi-mode optimum method is proved to be accurate and universal to different hydro-transient cases. Zhou et al. (2018) used simulated annealing algorithm to optimize the two-segment wicket gate closure law. In a practical case, two controlling conditions were selected in; the maximum volute pressure and maximum turbine speed numerical calculation, and result of different closure law were compared and analyzed. Lai et al.2019 used multi-objective artificial sheep algorithm (MOASA) is adopted to optimize the three-phase closure law of guide vanes. They concluded that proposed three-phase CLGV optimized using MOASA achieves significant superiority over the traditional one- or two-phase CLGVs.

2.6 Literature Gap

Most of the past research work are focused on optimization of two-phase closure law of guide vanes. Several researches have been done on optimization algorithm However, the three phase closure law has been rarely considered by the researcher. Moreover, very limited research has focused on the objective function of the optimization. The traditional linear objective function can ensure the target parameters within the permitted scope (Zhao et al., 2010).However, unlike non-linear objective function; it does not guarantee the better distribution of the safety margin of each target (Cui et al., 2013). Hence, this thesis focuses on the optimization of the parameters of a three-phase closure pattern for a typical operational hydropower plant of Nepal using non-linear objective function of pressure and speed rise.

CHAPTER THREE: RESEARCH METHODOLOGY

The sequence of operation that has been done in this thesis is shown in figure below:

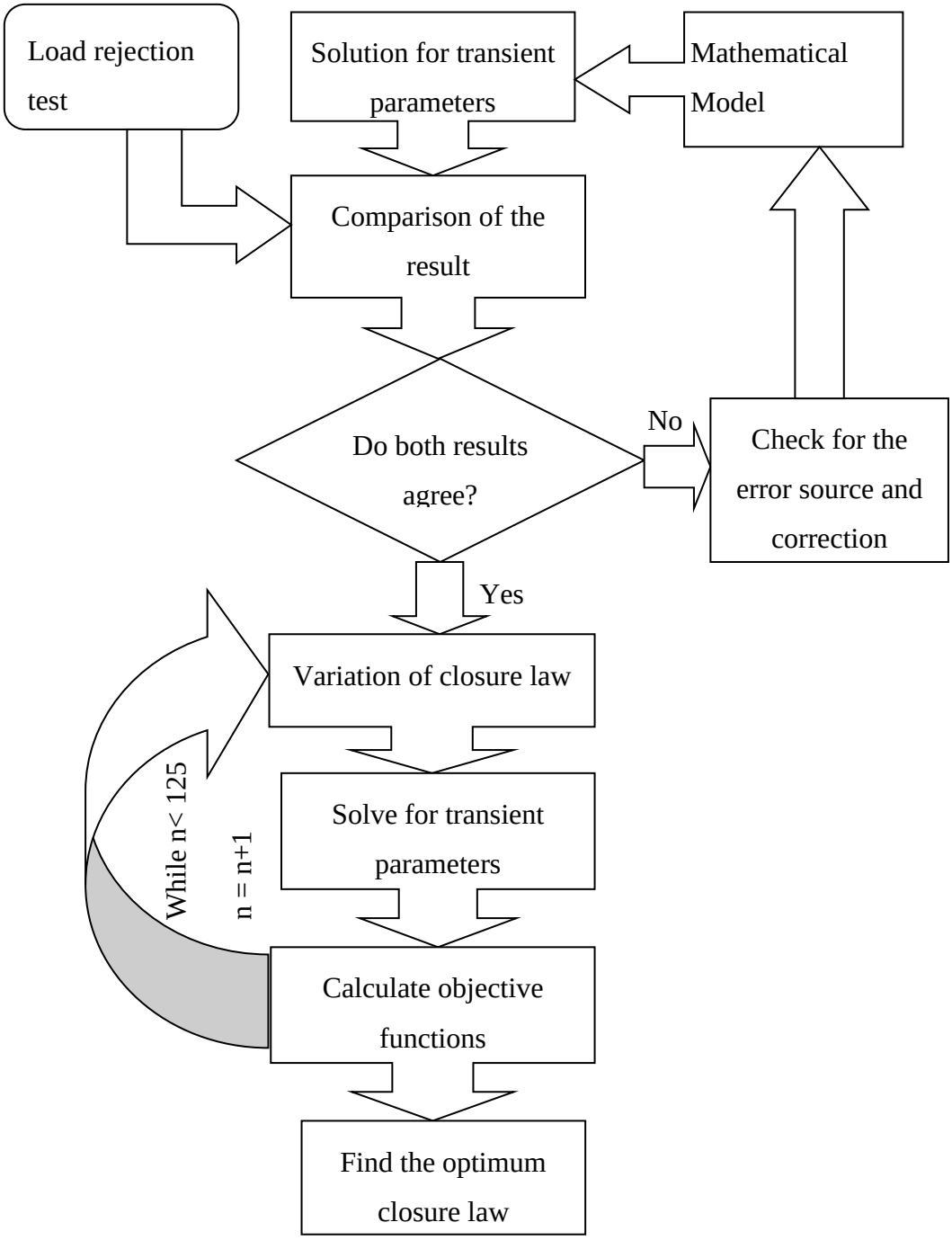

Figure 3. 1 Methodology of thesis

3.1 Mathematical Model Development

Mathematical model has been developed in commercial software Bentley HAMMER. HAMMER has been used by many researchers in the past to carry out the transient analysis in the water conveyance network (Turki, 2013; Desmukh, 2014; Saha, 2017). Bentley hammer uses the Methods of Characteristics to solve the one dimensional governing equation of water-hammer. The options for model development in Bentley Hammer includes but not limited to the following (Bentley, 2013):

a User can draw the network diagram and prepare one-dimensional model of the water conveyance system.

b User can define the closure and opening pattern of the valves and gates.

c User can select and define the hydraulic elements (surge tank, air valve, bypass valve, pipes, and turbine) whose boundary condition is in built modeled in the components.

d User can select the different friction models; static, quassi-static and unsteady .For unsteady friction model Vitkovsky approach has been employed.

e There is an option for the selection of either the wave speed adjustment or the grid spacing adjustment to match the CFL condition.

f Turbine has been modeled using Characteristics graph based iterative turbine model.

g The temporal and spatial variation of the pressure, flow, head, and the volume of the air-pockets can be obtained

h The temporal variation of rotational speed of the turbine can be obtained

3.1.1 Geometry setup

For the one dimensional analysis, the geometry of the waterway network is single line schematics representing the network and branches of the penstock pipe, surge shaft and tailrace. Figure 3.1 depicts the model that has been developed in BENTLEY HAMMER

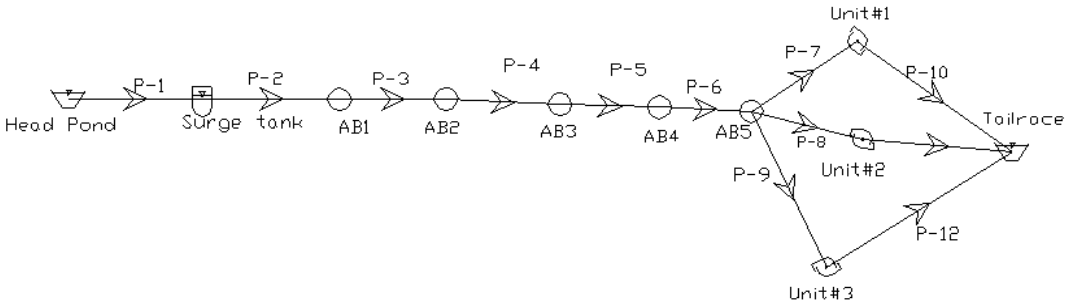

Figure 3. 2 Schematics of water conveyance network as built on BENTLEY HAMMER

Considering the effectiveness of computation, the length from surge tank to tailrace has been taken as the computational domain. The surge shaft of the hydropower station is simple-type surge shaft with thirty-five meter height and eight meter diameter. The penstock pipe is of mild steel which starts from the surge tank and extends up to the main inlet valve of the each unit. There are five anchor blocks and the trifurcation of the penstock occurs after the fifth anchor block. The elevation profile of the waterway network from the surge tank to the tailrace has been shown in fig 3.2.

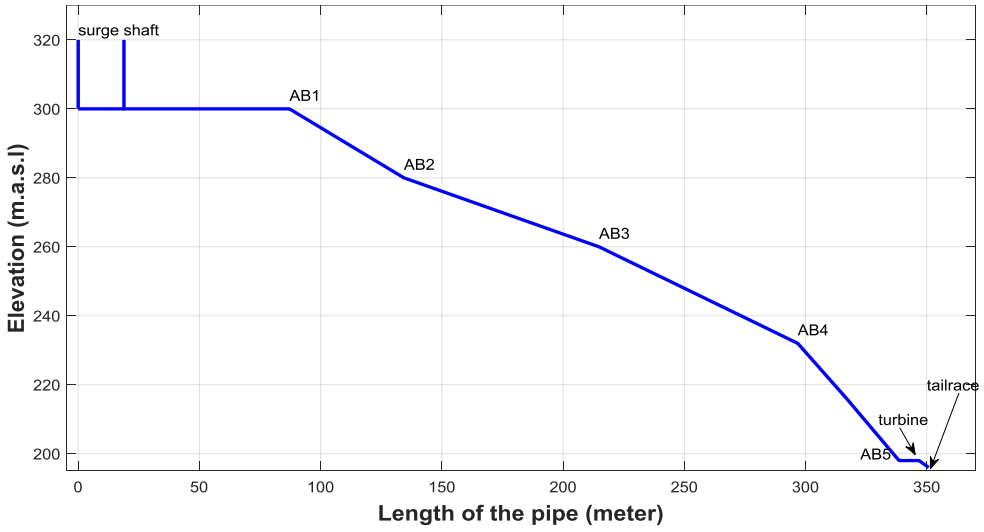

Figure 3. 3 Elevation profile of penstock pipe

Table 3. 1 Details of Physical properties of penstock pipe

Network Components	Diameter (mm)	Thickness (mm)	Length (meter)	Start point	Stop point
P2	2600	10	87.13	Surge shaft	AB01
P3	2600	12	47.2	AB-01	AB-02
P4	2600	16	80.46	AB-02	Ab-03
P5	2120	20	81.98	AB-03	AB04
P6	1500	25	20.136	AB04	AB05
P7	1500	25	21.66	AB5	Turbine Main Inlet Valve Unit 1
P8	1500	25	21.66	AB5	Turbine Main Inlet Valve Unit 2
P9	1500	25	21.66	AB5	Turbine Main Inlet Valve Unit 3

The hydropower station has three units, each having an installed capacity of 7.5 MW. The net head and net flow of each turbine is 108.23 meter and 24 cubic meters per second respectively. The rated rotational speed of the generator is 600 RPM and the rotating system has a combined moment of inertia of 31,000 kg.m^2.

3.1.2 Computational set up

The transient conditions have been modeled using transient solver of the Bentley Hammer. The unsteady friction model based on instantaneous acceleration has been employed .The wave speed varies at different section of the pipeline since it is dependent upon the physical property of the pipeline. The selection of grid spacing Δx is done on such a way that the CFL number is equals to one. To do the same, since, the wave speed is dependent upon the physical properties; the grid spacing has been adjusted for a defined time step. The time step has been selected based on the sensitivity analysis of the result on the time step. The selection of time step based on sensitivity analysis wills tradeoff between the accuracy of the result and the time taken to compute the solution. The computation has been done for the 3000 second time soon after the wicket gate closure is started.

3.1.3 Setting up closure pattern:

The numerical simulation has been done for the same closure pattern as did experimentally during the load rejection test, which was carried out during the commissioning phase of the project. The Main Inlet Valve (MIV) of each unit starts to operate once the guide vanes are fully closed and the closure time of MIV is sixty seconds. Hence, MIV is not supposed to have any pulsating effect of pressure in addition to the effect of guide vanes. The data of experimental load rejection test suggests that for the full rejection of load, the closure pattern of guide vane was single-stage linear and the closure speed was varied by rotating the knob of a throttle valve of the governor. The four variations in closure period were five, ten, fifteen and twenty seconds as shown in figure 3.4.

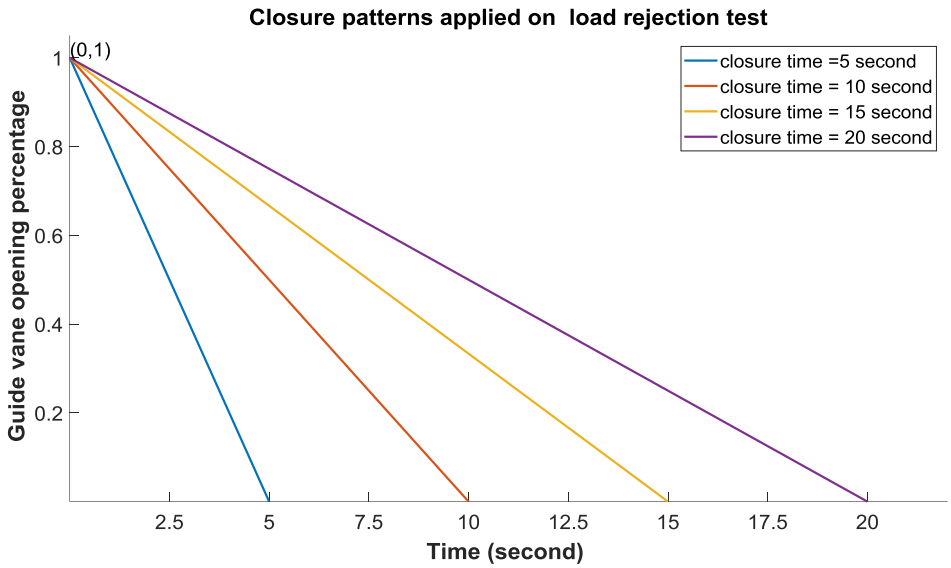

Figure 3. 4 Closure patterns applied on load rejection test

3.1.4 Solution for transient parameters:

The governing water hammer equation, the torque equation along with the turbine characteristics curve and closure pattern has been be employed to solve for the pressure, head, discharge and turbine rotational speed at different co-ordinate of time and position.

3.2 Validation of numerical model

The validation of the developed numerical model has been done by comparing the maximum value of pressure and maximum rotational speed of the turbine as obtained from numerical simulations with the data of the load rejection test.

3.3 Application of model for optimization of wicket gate closure law

The numerical model after validation has proved to be reliable for further operation and hence the model has been applied to find the optimum closure pattern of the guide vanes for a three-phase CDC pattern.

3.3.1 Optimization variables

The optimization variables are four free parameters describing the three-phase CDC closure pattern as shown in figure 2 ; time at which first closure stage finishes (t_1), time at which second stage closure starts (t_2), the fold point position (s) and the time at which the wicket gates are fully closed (t_3).

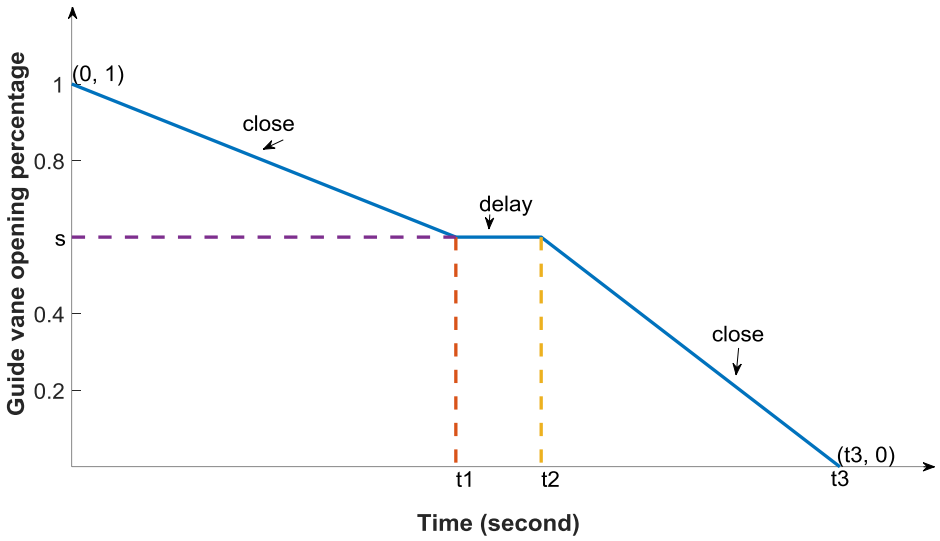

Figure 3. 5 Optimization variables for three phase CDC Closure pattern

3.3.2 Objective function

For the optimization, a non-linear objective function has been adapted from the research work of Cui et al. (2012).The objective function F has been defined as follows:

$$F = \frac{N_a - N_i}{N_a - N_{max}} \cdot \frac{P_a - P_i}{P_a - P_{max}}, \qquad \text{If} \quad N_{max} < N_a \ \text{AND} \ P_{max} < P_a$$

$$F = \infty \qquad \text{If} \quad N_{max} > N_a \ \text{OR} \ P_{max} > P_a \qquad \text{Equation 3.1}$$

The overall safety factor (SF) of the design is calculated as,

$$SF = \frac{P_a}{P_{max}} \frac{N_a}{N_{max}} \qquad \text{Equation 3.2}$$

Where,

N_a = Allowable maximum rotational speed of turbine (RPM)

N_{max} = Maximum rotational speed (RPM)

N_i = Rotational speed at initial steady state (RPM)

P_a = Maximum allowable pressure (KPA)

P_{max} = Maximum pressure (KPA)

P_i = Pressure at initial steady state (KPA)

SF = Overall safety factor of the system

The denominator of the objective function contains the product of two terms, each representing the difference of the maximum and allowable value of each sub-goal. Hence, it is supposed that the optimum solution based on this objective function will uniformly distribute the safety margin of each objective goal compared to the conventional linear objective function.

The value of initial steady-state pressure has been calculated by using a steady-state solver of Bentley hammer software. For the consideration of safety, the maximum allowable values of speed and pressure are set as Na = 900 RPM and Pa = 1800 KPA.

3.3.3 Optimization algorithm

The numerical simulation has been repeatedly done by varying one variable at once. The t_2 and t_1 have been related by the defined relationship. The remaining three variables; t1, t3 and s, each has been provided five variations over the uniform interval, accounting for a total of one hundred and twenty-five combinations of t1,t2, t3 and s. The value of maximum pressure and maximum rotational speed calculated for each combination are used to evaluate the objective function. The combination of t1, t2, t3 and s which gives the minimum value of the objective function has been considered as optimum parameters for a two-stage closure pattern. The value of objective function for optimum parameters is then compared with the optimum parameters of single-stage linear closure pattern.

CHAPTER FOUR: RESULTS AND DISCUSSION

4.1 Numerical simulation for single-staged closure pattern

4.1.1 Valve closure time: 5 sec

The results of numerical simulation for the single-stage linear closure pattern with closure period t = 5 seconds, has been shown in figure 4.1, figure 4.2, figure 4.3 and figure 4.4. The spatial variation of pressure along the longitudinal section of penstock pipe considering the start of the spiral casing as x=0 has been shown in figure 4.1.The red, green and blue lines in the figure indicates maximum, initial and minimum pressures respectively. The figure shows that the maximum pressure is observed at the start of the spiral casing. The temporal variation of the pressure at the same position has been shown in figure 4.2. The result shows that the pressure increases steeply till the time t = 5 seconds and fluctuation starts. The fluctuation gradually dampens which has been shown in figure 4.3. From figure 4.2 and figure 4.3 it can be seen that the value of maximum pressure along the entire pipeline is 1722 KPA which is observed on start of spiral casing at time t = 13 second. Figure 7 shows the temporal variation of the rotational speed of the turbine for closure time t= 5 seconds. The result shows that speed rises rapidly soon after the load rejection. The maximum value of the rotational speed is 722 RPM.

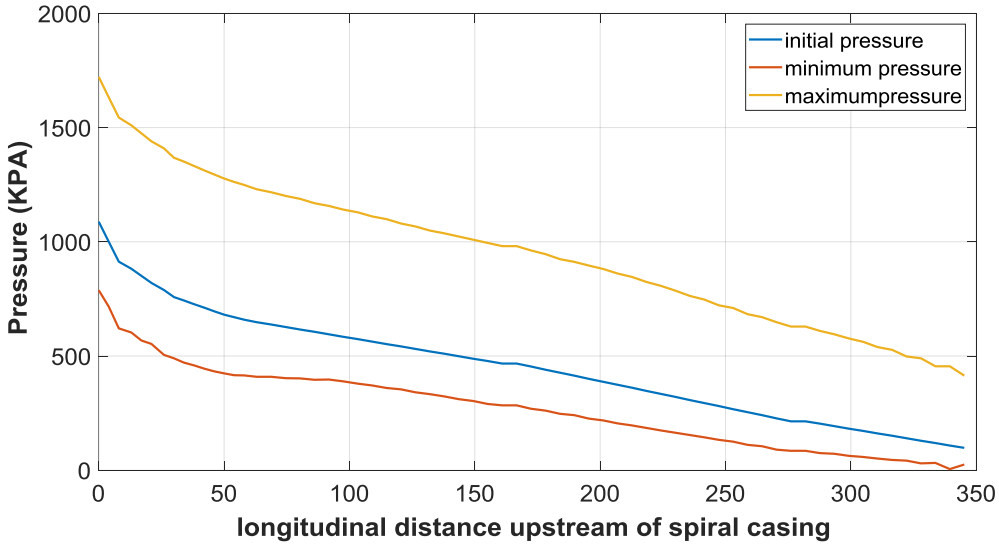

Figure 4. 1 Pressure variation along the penstock pipe, $t_{closure}$ =5 second

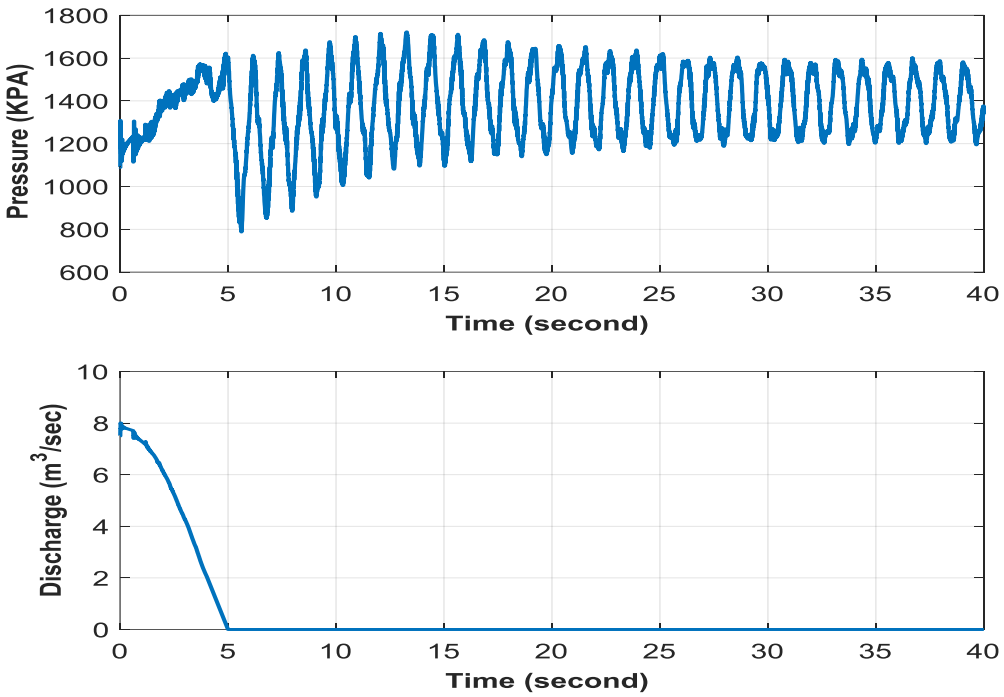

Figure 4. 2 Temporal variation of pressure and flow at spiral casing, t =5 second

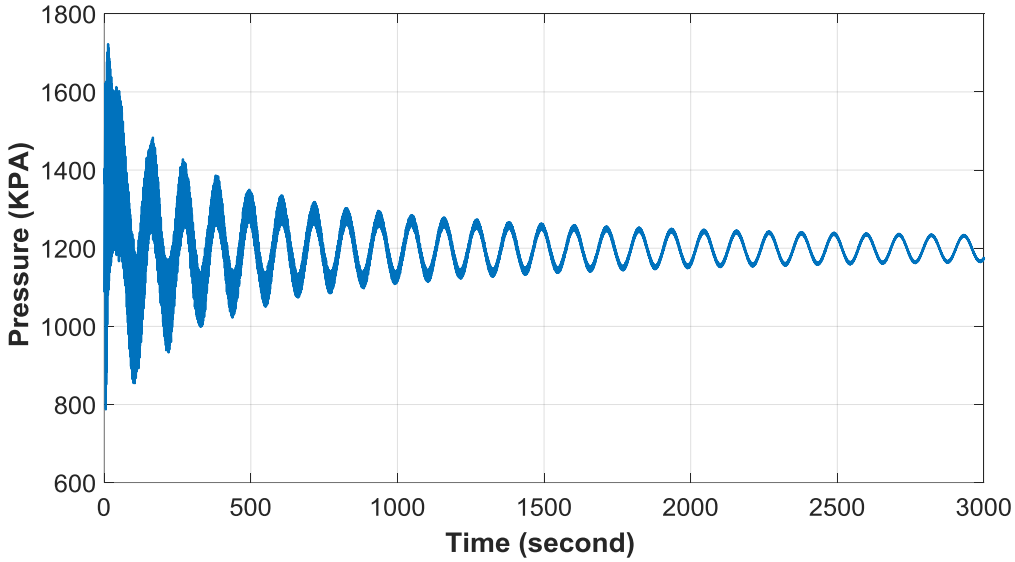

Figure 4. 3 Damping of pressure at spiral casing, t= 5 second

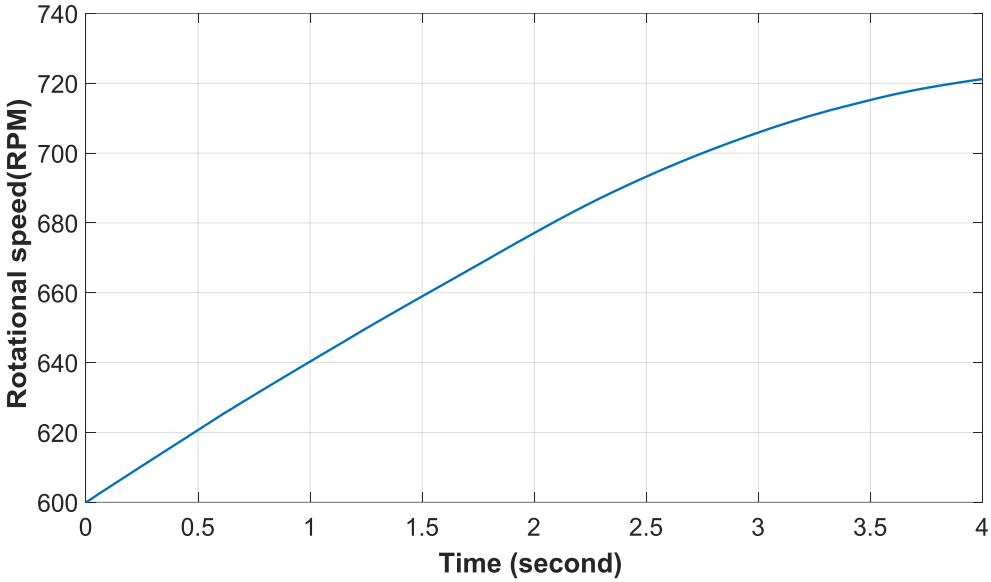

Figure 4. 4 Temporal variation of rotational speed of runner, t= 5 second

4.1.2 Valve closure time: 10 sec

The results of numerical simulation for the single-stage linear closure pattern with closure period t = 10 seconds, has been summarized in figure 4.4, figure 4.5, figure 4.6 figure 4.8. The spatial variation of pressure along the longitudinal section of penstock pipe considering the start of the spiral casing as x=0 has been shown in figure 4.5.The red, green and blue lines in the figure indicates maximum, initial and minimum pressures respectively. The figure shows that the maximum pressure is observed at the start of the spiral casing. The temporal variation of the pressure at the same position has been shown in figure 4.6. The result shows that the pressure increases steeply till the time t= 10 seconds and fluctuation starts. The fluctuation gradually dampens which has been shown in figure 4.7. From figure 4.5 and figure 4.7, it can be seen that the value of maximum pressure along the entire pipeline is 1525 KPA which is observed on start of spiral casing at time t = 17.52 second. Figure 4.8 shows the temporal variation of the rotational speed of the turbine for closure time t= 10 seconds. The result shows that speed rises rapidly soon after the load rejection. The maximum value of the rotational speed is 792 RPM.

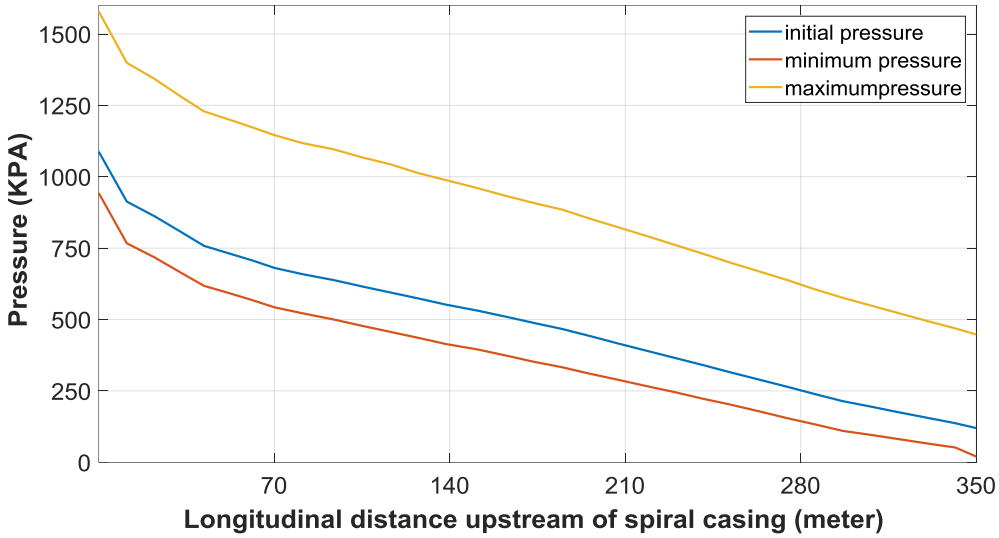

Figure 4. 5 Pressure variation along the penstock pipe, $t_{closure}$= 10 second

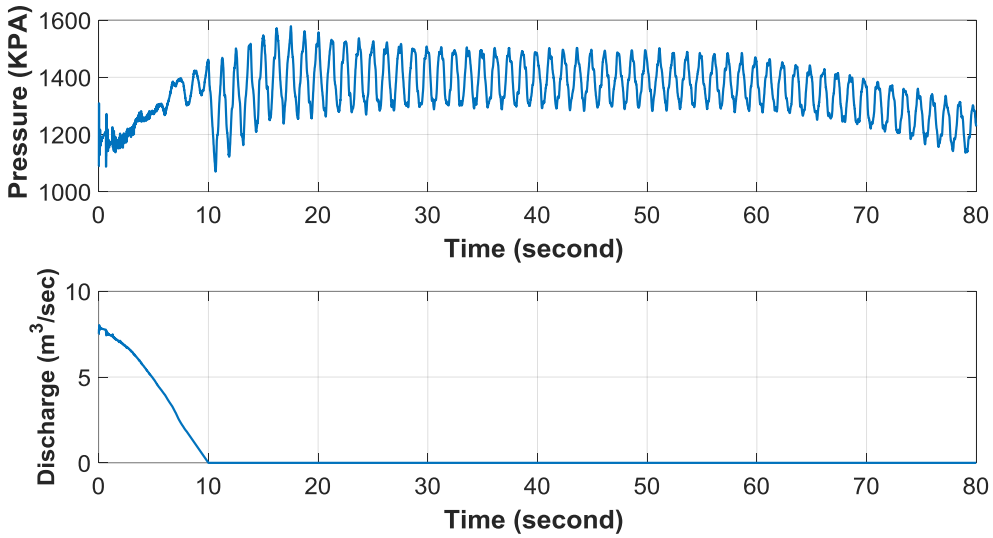

Figure 4. 6 Temporal variation of pressure and flow at spiral casing, $t_{closure}$= 10 second

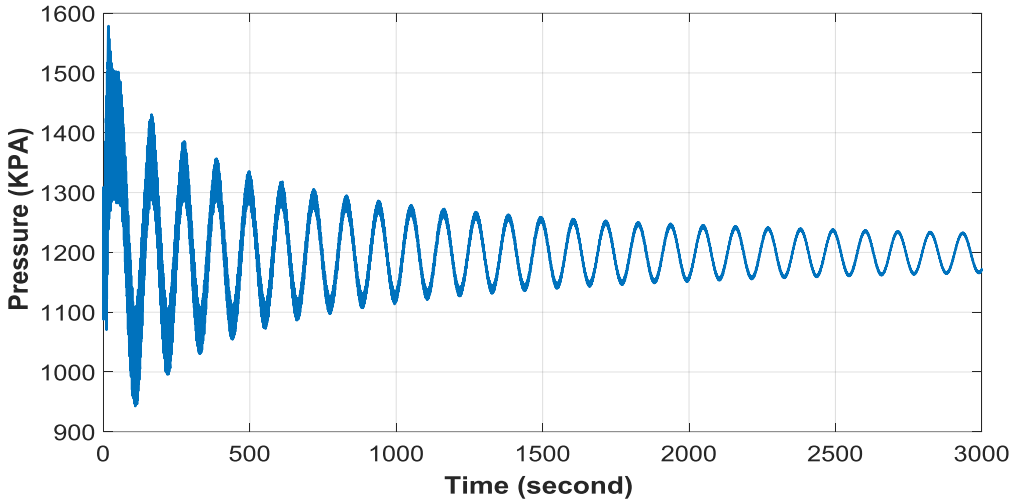

Figure 4. 7 Damping of pressure at spiral casing, $t_{closure}$= 10 second

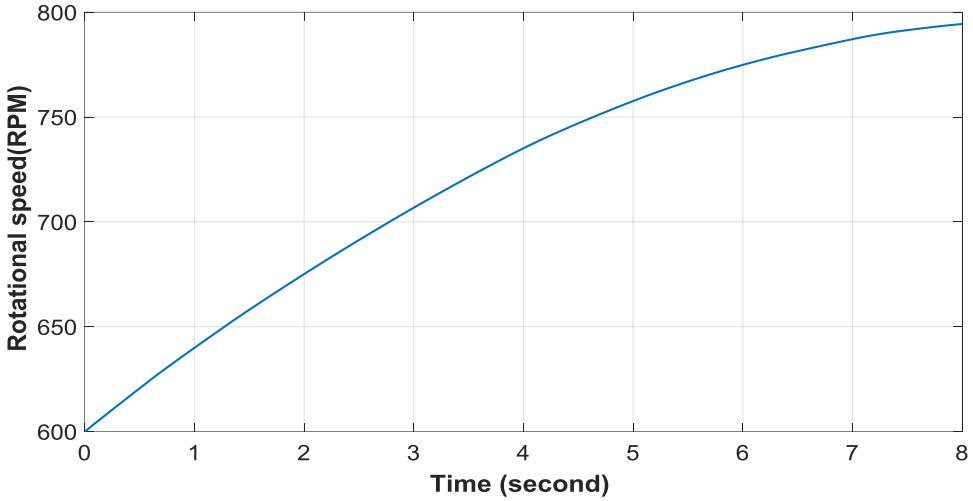

Figure 4. 8 Temporal variation of rotational speed of runner, $t_{closure}$= 10 second

4.1.3 Valve closure time: 15 sec

The results of numerical simulation for the single-stage linear closure pattern with closure period t = 15 seconds, has been summarized in figure 4.9, figure 4.10, figure 4.11 and figure 4.12. The spatial variation of pressure along the longitudinal section of penstock pipe considering the start of the spiral casing as x=0 has been shown in figure 4.9.The red, green and blue lines in the figure indicates maximum, initial and minimum pressures respectively. The figure shows that the maximum pressure is observed at the start of the spiral casing. The temporal variation of the pressure at the same position has

been shown in figure 4.10. The result shows that the pressure increases steeply till the time t = 15 seconds and fluctuation starts. The fluctuation gradually dampens which has been shown in figure 4.11. From figure 9 and figure 11, it can be seen that the value of maximum pressure along the entire pipeline is 1512 KPA which is observed on start of spiral casing at time t = 18.8 second. Figure 4.12 shows the temporal variation of the rotational speed of the turbine for closure time t= 15 seconds. The result shows that speed rises rapidly soon after the load rejection. The maximum value of the rotational speed is 845 RPM.

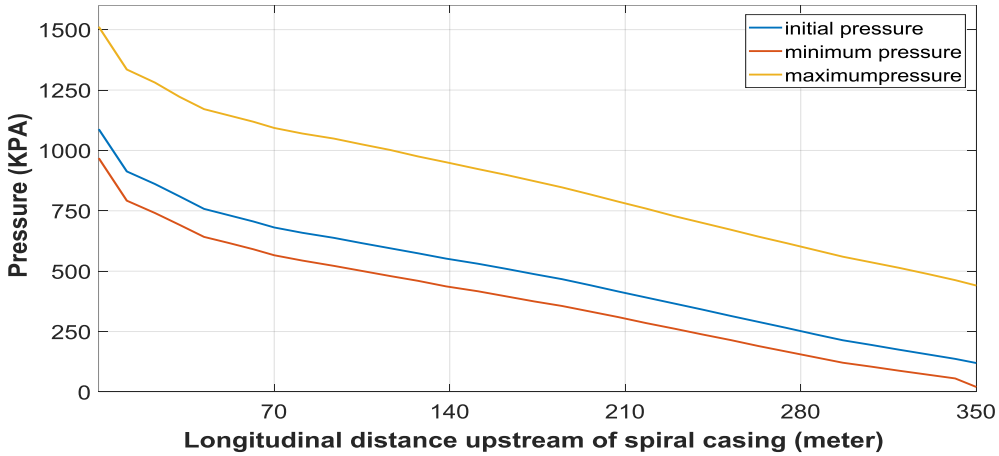

Figure 4. 9 Pressure distribution along the penstock pipe, tclosure = 15 second

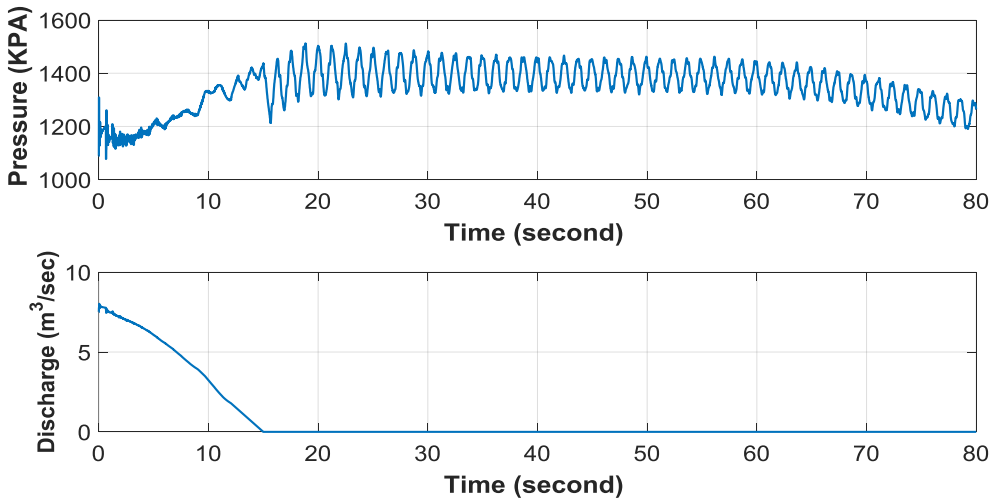

Figure 4. 10 Temporal variation of pressure and flow at inlet of spiral casing, $t_{closure}$= 15 second

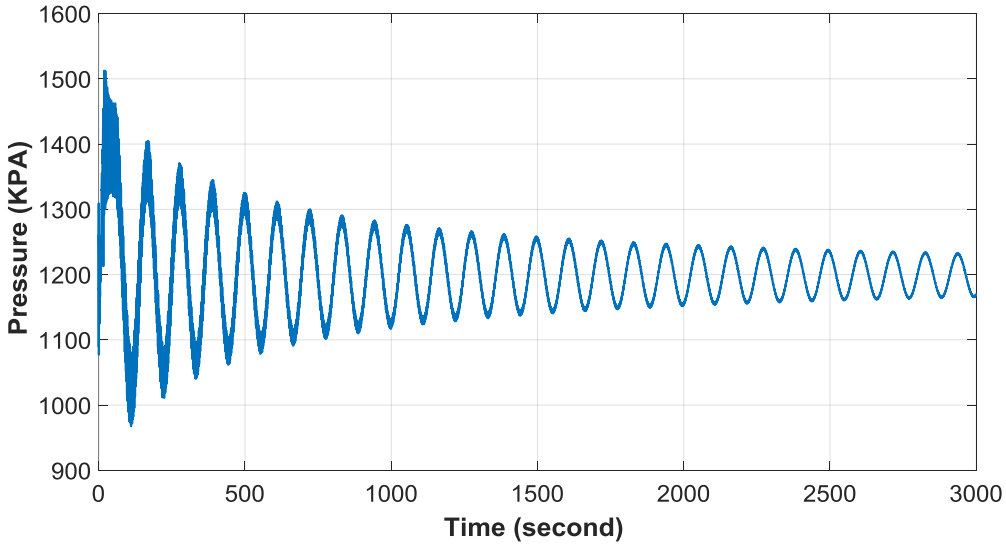

Figure 4. 11 Pressure damping at inlet of spiral casing, $t_{closure}$ = 15 second

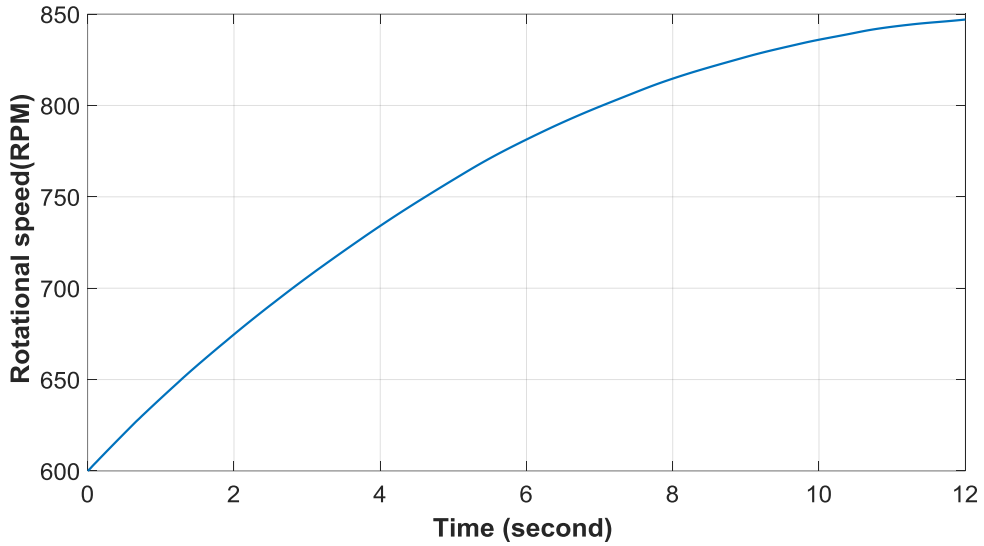

Figure 4. 12 Temporal variation of rotational speed of runner, $t_{closure}$= 15 second

4.1.4 Valve closure time: 20 sec

The results of numerical simulation for the single-stage linear closure pattern with closure period t = 5 seconds, has been summarized in figure 4.13, figure 4.14 figure 4.15 and figure 4.16. The spatial variation of pressure along the longitudinal section of penstock pipe considering the start of the spiral casing as x=0 has been shown in figure

4.13.The red, green and blue lines in the figure indicates maximum, initial and minimum pressures respectively. The figure shows that the maximum pressure is observed at the start of the spiral casing. The temporal variation of the pressure at the same position has been shown in figure 4.14. The result shows that the pressure increases steeply till the time t=20 seconds and fluctuation starts. The fluctuation gradually dampens which has been shown figure 4.15. From figure 4.13 and figure 4.15, it can be seen that the value of maximum pressure along the entire pipeline is KPA which is observed on start of spiral casing at time t= 21.31 second. Figure 4.16 shows the temporal variation of the rotational speed of the turbine for closure time t= 20 seconds. The result shows that speed rises rapidly soon after the load rejection. The maximum value of the rotational speed is 886 RPM.

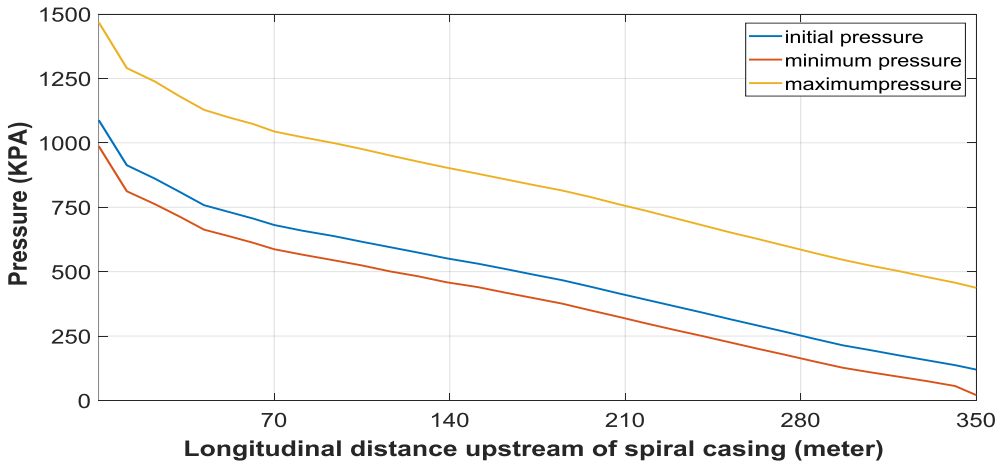

Figure 4. 13 Pressure at spiral casing tclosure =20 second

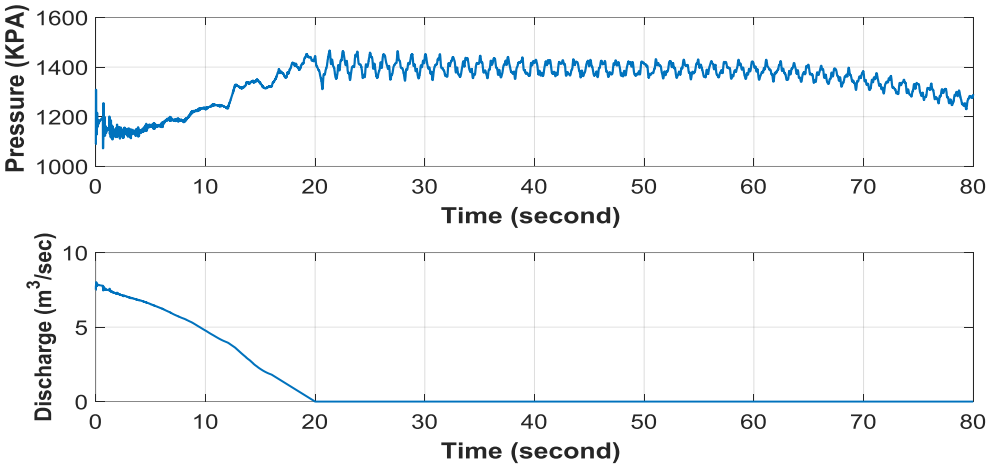

Figure 4. 14 Temporal variation of pressure and flow at the inlet of spiral casing, $t_{closure}$=20 second

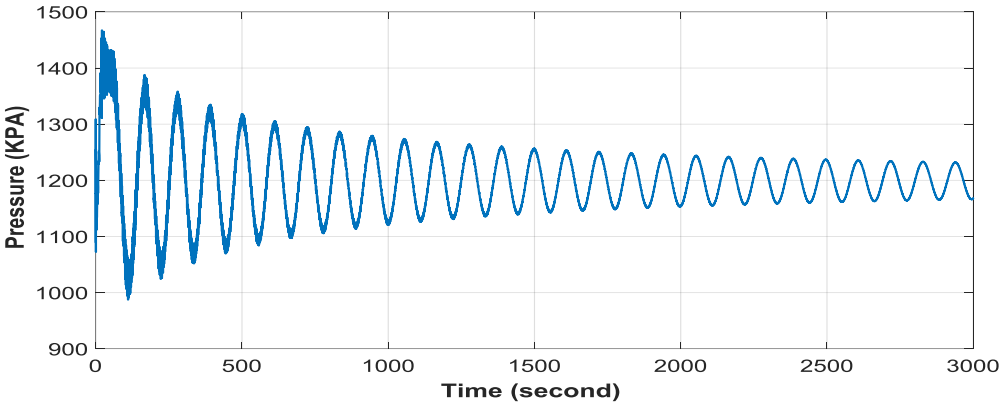

Figure 4. 15 Damping of pressure, $t_{closure}$ = 20 second

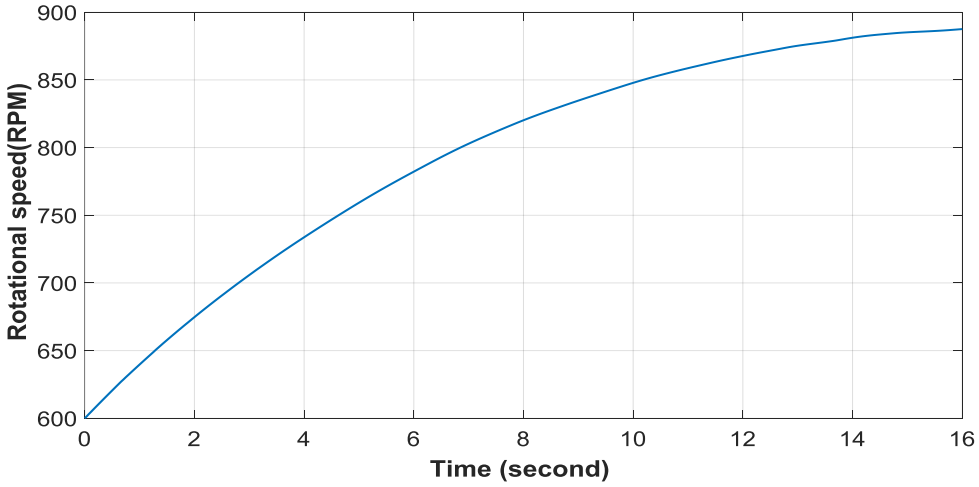

Figure 4. 16 Temporal variation of rotational speed of turbine $t_{closure}$ = 20 second

4.2 Experimental results

Following is the summary of experimental data for 100% load rejection test which were carried out during commissioning period of Sanima Mai Hydropower project. The data has been extracted from commissioning report as provided by Sanima Mai Hydropower Limited.

Table 4. 1 Results of experimental load rejection test

Closure Time (Sec)	Speed (RPM)			Maximum Pressure		
	Before Load rejection	After load rejection	Percentage Increase	Before Load rejection	After Load rejection	Percentage Increase
5	600	715	19%	1198	1750	46%
10	600	770	28%	1198	1610	34%
15	600	830	38%	1198	1543	29%
20	600	870	45%	1198	1510	26%

4.3 Comparison of results

Table 4. 2 Comparison of results of numerical simulation and experiment

Closure Time (sec)	Maximum hydrodynamic pressure (KPA)			Maximum Rotational Speed (RPM)		
	Numerical simulation	Load rejection test	Discrepancy (%)	Numerical simulation	Load rejection test	Discrepancy (%)
5	1722	1780	3.25	722	715	-0.98
10	1580	1632	3.18	792	780	-1.54
15	1525	1567	2.68	845	830	-1.80
20	1496	1535	2.54	886	875	-1.26

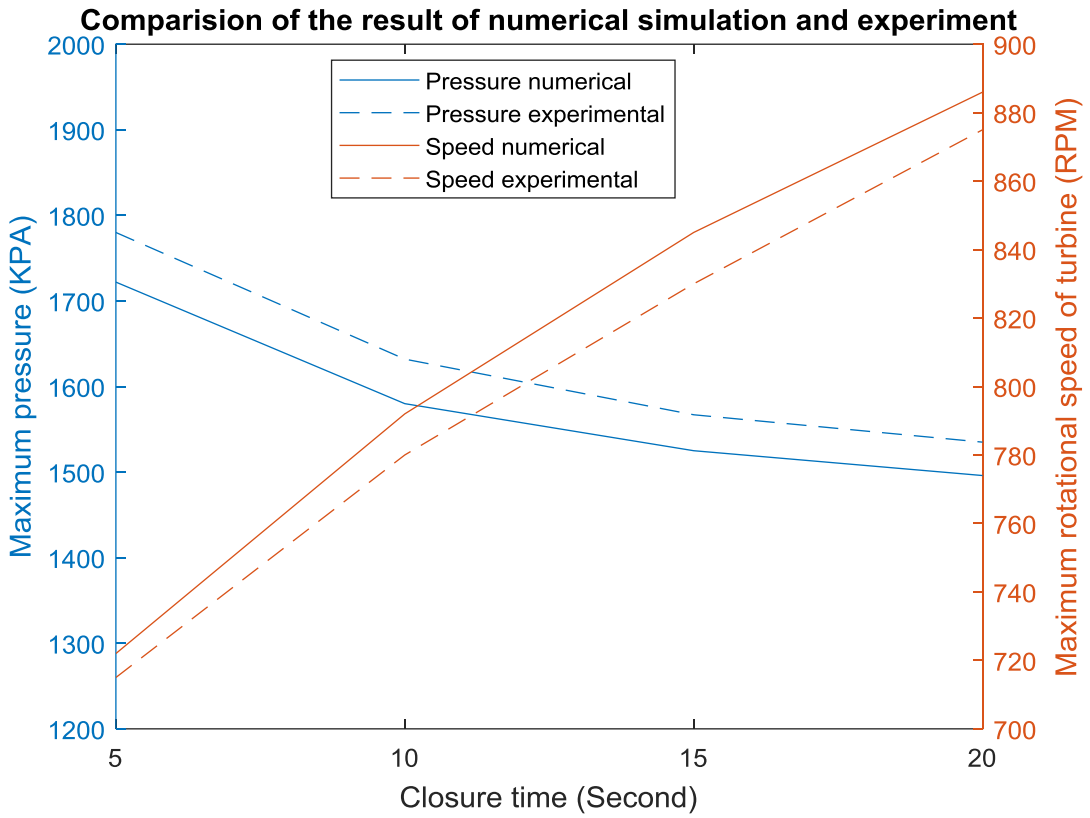

Figure 4. 17 Comparison of results of numerical simulation and experiment

Figure 4.17 demonstrates the comparison results between the data collected in field test and the numerical calculation. The comparison of results indicates that the maximum deviation of numerical simulation and the experimental test is 3.2 percent, which suggests that the mathematical model of transient process is valid and reliable.

4.4 Optimization of the closure pattern

4.4.1 Single phase linear closure pattern

Table 4.3 summarizes the result of numerical simulation with different closure time. Figure 4.17 shows the variation of objective function with respect to the closure time. From the figure it is seen that the objective function is minimized at $t_{closure}$ = 7 second and the corresponding value of objective function is 6.415. The overall safety factor of the design for optimum closure is 1.39.

Table 4. 3 Results of various closure law of Single-phase linear closure pattern

Closure time (Second)	Maximum Pressure (KPA)	Maximum Rotational speed (RPM)	Objective function
5	1722	722	17.286
6	1661	740	10.791
7	1542	755	6.415
8	1554	766	7.281
9	1565	782	8.655
10	1580	792	10.101
11	1534	806	9.598
12	1491	817	9.358
13	1473	828	10.194
14	1501	838	12.946
15	1525	845	15.868
16	1509	856	18.744
17	1484	865	21.700
18	1484	873	28.129
19	1461	880	35.398
20	1496	886	56.391

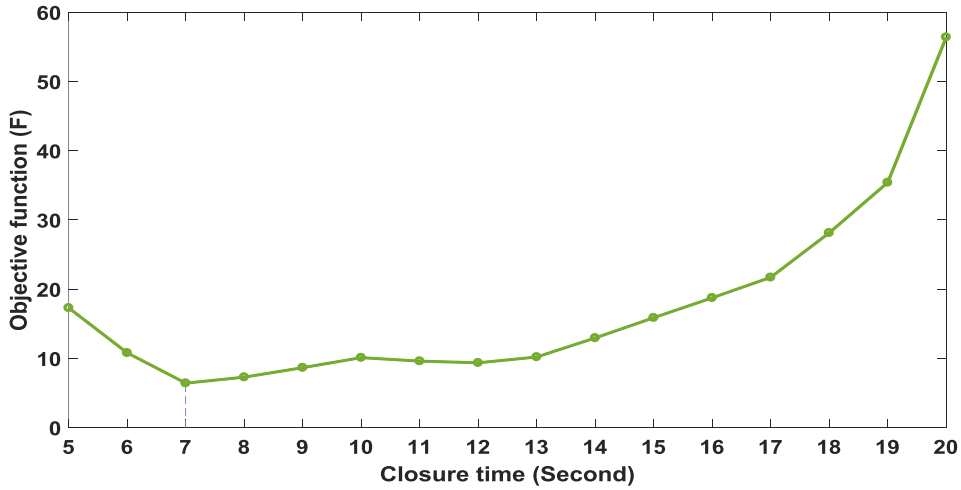

Figure 4. 18 Variation of objective function with closure time

4.4.2 Three phase CDC Closure pattern

As noted previously, there are four factors that can affect the transient process: time at which first closure stage finishes (t_1), time at which second stage closure starts (t_2), the fold point position (s) and the time at which the wicket gates are fully closed (t_3).The results of numerical simulations for a different combination of these four optimization variables have been presented in Table A.1. The optimized value of t_1, t_2, t_3, and s, based on one hundred and twenty-five simulations are 4 seconds, 5 seconds, 9 seconds, and 0.35 respectively. The corresponding values of the maximum pressure, maximum rotational speed and the objective function are 1507 KPa, 754 RPM, and 5.61 respectively. The overall safety factor of design for the optimum closure is 1.425.

Fig 4.19 shows the individual effect of the variation of the four parameters t_1, t_2, t_3 and s on the maximum rotational speed of turbine. When plotting the figure, one of the factors is changed while the other three are fixed. Figure shows that maximum speed increases on increasing any of the four parameters; t_1, t_2, t_3 and s, provided that the remaining three variables remains unchanged.

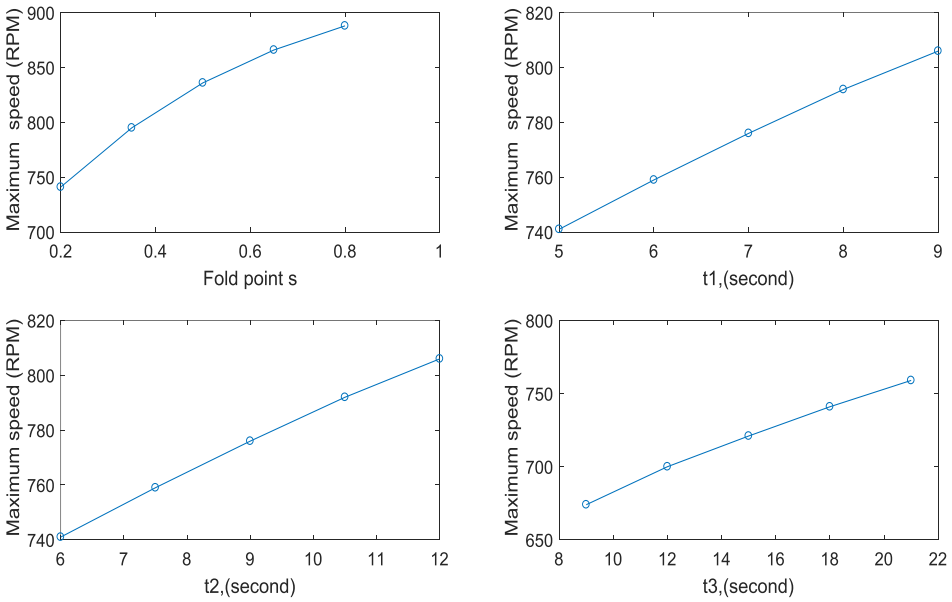

Figure 4. 19 Relationship between the Maximum rotational speed and the parameters of three-phase CDC pattern

In a similar way, figure 4.20 shows the individual effect of the variation of the parameters t_1,t_2, t_3 and s on the maximum pressure. Except for the case of full closure

time t_3, there is no any clear trend observed in the relation between maximum pressure and these three variables.

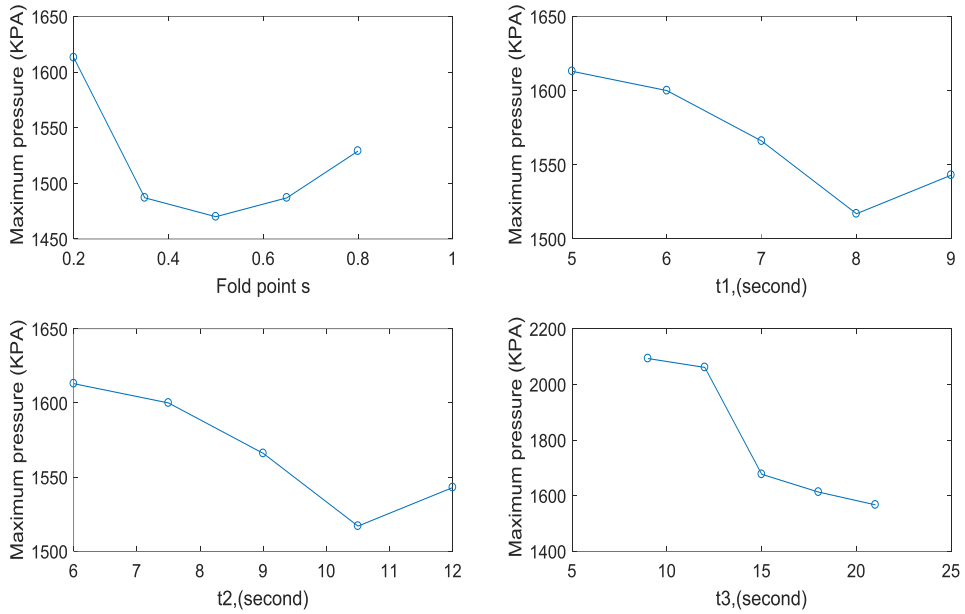

Figure 4. 20 Relationship between the maximum pressure and the parameters of three-phase CDC pattern

The plot of the objective function versus the difference of slope of first and second closure is in figure 4.21.

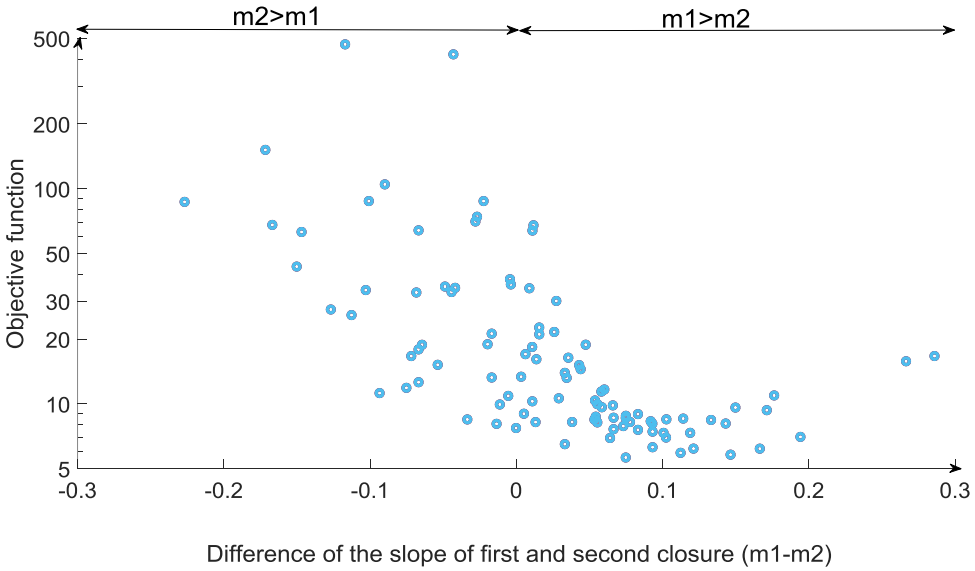

Figure 4. 21 Graph of the difference of the slope of first and second closure versus objective function

Figure 4.21 contains the two regions which are $m_1 > m_2$ and $m_2 > m_1$. Comparing the value of objective function in both the sides, it is obvious that the better value of objective function is obtained when $m_1 > m_2$, i.e., when the first closure is steeper than second closure. Hence, to better contradict the rise of rotational speed and pressure, the designer should always choose the closure pattern in such a way that the speed of first closure is faster than second closure.

CHAPTER FIVE: CONCLUSIONS AND RECOMMENDATIONS

5.1 Conclusion

This thesis work deals with the development of mathematical model of hydraulic transients for a typical medium head hydropower plant. The correctness of results of the mathematical model has been validated in comparison with the experimental data. The maximum discrepancy of the numerical and experimental result has found to be 3.2%, which concludes that the numerical model can predict the parameters of hydraulic transient with satisfactory accuracy. The validated model has been employed to optimize the closure pattern of guide vanes for the same hydropower plant Various combinations of single-phase linear and three-phase close-delay-close (CDC) closure patterns have been applied to the validated model to study the effect of the closure pattern. The value of maximum hydrodynamic pressure and the maximum rotational speed of turbine are calculated for all the cases of guide vane closure. To quantify the effectiveness of a closure pattern to harmonize the rise of hydrodynamic pressure and the rotational speed of turbine, a non-linear objective function has been proposed and based on the extent of the minimization of the defined objective function, different closure laws are compared. For a single-phase closure law, the maximum pressure decreases and the maximum speed increases on increasing the closure time and vice-versa. The optimum closure law for single phase linear closure pattern is obtained at closure time of seven seconds which keeps the maximum pressure and maximum speed at 1542 KPA and 755 RPM respectively .The corresponding value of objective function is 6.4.

For a three-phase CDC pattern, maximum speed increases on increasing any of the four parameters; t_1, t_2, t_3 and s, provided that the remaining three variables remains unchanged. However, there are no any clear trends observed for the maximum pressure. Nevertheless, it has been concluded that the value of objective function is better controlled when the speed of first closure is faster than the speed of second closure. The optimum closure law for a three phase CDC pattern is obtained at t_1= 4 second, t_2= 5 second, t_3 = 9 second and s= 0.35 which keeps the maximum pressure and maximum

speed at 1507 KPA and 754 RPM respectively. The corresponding objective function is 5.6.

The optimum closure law obtained in both the pattern ensures the target hydraulic transient parameters within the defined range. Moreover, the comparison of the value of objective function for single phase and three phase CDC linear closure pattern concludes that the three-phase CDC pattern ensures better regulation than the single phase closure pattern.

The achievement of this study can be a reference for similar projects.

5.1 Recommendations

The thesis recommends the following possible research work for continuation in the future:

a) The effectiveness of three-phase Close-Delay-Close pattern to harmonize the extreme conditions of pressure and speed can be compared with the effectiveness of three-phase Close-Reopen-Close and three-phase Close-Close-Close pattern.

b) Comparison of wave shape, maximum value and the time of the maximum value of the pressure and speed between numerical simulation and experimental data will better corroborate the validity of result of the numerical simulation.

REFERENCES

Adamkowski Adam (2001). Case Study : Lapino Powerplant Penstock Failure . *Journal of Hydraullic Engineering-ASCE,127,547-555*

Ali Rezghi, A. R. (2015). Sensitivity Analysis of Transient Flow of Two Parallel Pump-Turbines Operating at Runway. *Renewable Energy, 86*.

Alireza Riasi, P. T. (2017). Numerical Analysis of the hydraulic transient response in the presence of surge tanks and relief valves. *Renewable Energy, 107*, 138-146.

Anton Bergant, B Karney, S Pejovic,J Mazij, ed. "Treatise on water hammer in hydropower standard and guidelines." IOP Conference Series: Earth and Environmental Science. IAHR Symposium on hydraulic machinery and system, 2014.

Anton Bergant, A. K. (2012). *Strojniski Vestnik-Journal of Mechanical Engineering, 58*, 225-237.

Anton Bergant, A. R. (2001). Development in Unsteady pipe flow friction modelling. *Journal of Hydraulic Research, 39*(3), 249-257.

Benjamin Wylie, L. S. (1993). *Fluid Transients in Systems.* Englewood Cliff: Prentice Hall.

Bentley. (2013). Retrieved October 24, 2019, from Bentley:

http://docs.bentley.com/

Carlsson, J. (2016). *Water Hammer Phenomenon Analysis using the Method of Characteristics and Direct Measurements using a "stripped" Electromagnetic Flow Meter.* Royal Institute of Technology, Division of Nuclear Reactor Technology, Department of Physics. Royal Institute of Technology.

Chaudhry, M. H. (2014). *Applied Hydraulic transient* (3rd ed.). Springer.

Chaudhry M.H. and Hussaini M.Y. (1985). Second–order accurate explicit finite–difference schemes for wate rhammer analysis. Journal of Fluid Engineering 107(4), 523 - 529

Chen Sheng, J. J. (2013). Optimization of two-stage closure law of wicket gate and application. *Applied Mechanics and materials*, 636-641.

Cui, H. F. (2012). Optimization of wicket gate closing law considering different case. *IAHR Symposium on hydraulic machinery and system. 15.* IOP Conference series: Earth and Environmental Science.

Deshmukh, T. (2014). Hydraulic transient analysis of Kolar Water pipeline using Bentley Hammer V8i-A Case Study. *Internal Journal of research and technology, 3*(9), 1-3.

G., P. (2000). Local balance unsteady friction model. *Journal hydraulic engineering*, 45-56.

Guangtao Zhang, Y. C. (2015). Research on Francis Turbine Modelling for Large Disturbance Hydropower station Transient Process Simulation. *Mathematical Problems in Engineering*, 1-10.

Helena Ramos, D. C. (2004). Surge damping analysis in pipe systems: modelling and experiments. *Journal of Hydraulic Research, 42*(4), 413-425.

Jha,R,(2010). Total Run of the River Hydropower Potential of Nepal. *Hydro Nepal Journal ,2010(7)*

Mohamed S Ghidaoui, M. Z. (2005). A Review of water hammer theory and practice. *Applied Mechanics review*, 49-58.

Pezzinga, G. (2009). *Local Balance Unsteady Friction Model* (Vol. 135). Journal of Hydraulic Engineering.

Riasi, A. (2010). Influence of surge tank on fluid transient simulation in hydroelectric power plant using unsteady friction.

Saha, B. (2016). *Transient analysis of Pirulia Piped Water Supply Line Using Hammer Software.* Jadavpur University.

Sharif F, Siosemarde M, Merufinia E, Esmat Saatlo M. "Comparative Hydraulic Simulation of Water Hammer in Transition Pipe Line Systems with." Journal of Civil Engineering and Urbanism 4.3 (2014): 282-286.

Tijsseling, A. (1996). Fluid- structure interaction in liquid-filled pipe systems: a review. *Journal of fluids and structure*, 109-146.

Triki, A. (2017). Water hammer control in pressurized-pipe flow using a branched polymeric penstock. *Journal of Pipeline System Engineering and Practice, 8*.

Trivedi Chirag, B. G. (2013). Ëffect of transients on Francis Turbine runner life. *Journal of hydraulic research*.

Turki, A. E. (2013). *Modelling of Hydraulic Transient in Closed Conduits.* Department of Civil and Environmental Engineering. Colorado State University.

Urbanowicz, K. (2017). Computational compliance criteria in water hammer modelling. *E3S Web of Conferences, International Conference Energy, Environment and Material Science. 19.* EDP Sciences.

Victoria Bonath, M. L. (2009). *Numerical study on the characterctics of transient flow in Jinping II hydropower station with differential surge shaft.* Master's Thesis, Lulea University of Technology, Mining and Geotechnical Engineering.

Viktor Iliev, B. I. (2015). Sensitivity of transient phenomena analysis of the Francis turbine Power Plant. *International Journal of Engineering Research and Application*, 265-273.

Watters, G.Z. (1984). Analysis and control of unsteady flow in pipelines. 2ndedition, Butterworth−Heinemann, USA

Wei Zeng, J. Y. (2015). Guide-vane Closing Scheme for Turbines Based on Transient Characterctics in S-Shaped region. *Journal of Fluid Engineering, 138*(5).

Weiguo Zhao, L. W. (2010). Chinese Control and Decision Conference., (pp. 3552-3556).

Wuyi Wan, B. J. (2018). Investigation of water hammer protection in water supply pipeline system using an intelligent self-controlled surge tank. *Energies, 11*(6).

Xiaoqin Li, J. C. (2013). Wicket gate closure control law to improve the transient of a water. *Advanced Material and Research, 732-33*, 451-456.

Xinjie Lai, C. L. (2019). Multi-Objective Optimization of Closure law of Guide Vanes for Pumped-Storage Units. *Renewable Energy, 139*, 302-312.

Zhou, T. &. (2018). Optimizing closure law of wicket gates in hydraulic turbine based on simulated annealing. *Journal of Drainage and Irrigation Machinery Engineering, 36*, 320-326.

PUBLICATION

Title	: Optimization of Closure Law of Guide Vanes for an Operational Hydropower Plant of Nepal
Name of Journal	: International Journal of Engineering and Management Research
Authors	: Saroj Chalise and Laxman Poudel
Published Year	: 2019
Volume	: 9
Issue	: 5
e-ISSN	: 2250-0758
p-ISSN	: 2394-6962
DOI	: https://doi.org/10.31033/ijemr 9.5.12
Page number	: 73-79

APPENDICES

Appendix A: Results of numerical simulation for various combination of parameters of three-phase CDC closure pattern

Closure Law $[t_1,t_2,t_3,s]$	Slope of first closure	Slope of second closure	Maximum pressure at spiral casing (Kpa)	Maximum Rotational speed of turbine (RPM)	Objective function
[5, 6, 18,0.2]	0.160	0.017	1613	741	8.072
[5, 6, 18,0.35]	0.130	0.029	1487	795	7.303
[5, 6, 18,0.5]	0.100	0.042	1470	836	11.364
[5, 6, 18,0.65]	0.070	0.054	1487	866	22.552
[5, 6, 18,0.8]	0.040	0.067	1529	888	73.801
[6, 7.5, 18,0.2]	0.133	0.019	1600	759	8.511
[6, 7.5, 18,0.35]	0.108	0.033	1485	811	8.561
[6, 7.5, 18,0.5]	0.083	0.048	1500	851	16.327
[6, 7.5, 18,0.65]	0.058	0.062	1495	878	35.768
[6, 7.5, 18,0.8]	0.033	0.076	1514	898	419.580
[7, 9, 18,0.2]	0.114	0.022	1566	776	8.271
[7, 9, 18,0.35]	0.093	0.039	1486	826	10.329
[7, 9, 18,0.5]	0.071	0.056	1482	864	20.964
[7, 9, 18,0.65]	0.050	0.072	1525	890	87.273
[7, 9, 18,0.8]	0.029	0.089	1508	908	infinity
[8, 10.5, 18,0.2]	0.100	0.027	1517	792	7.852
[8, 10.5, 18,0.35]	0.081	0.047	1496	840	13.158
[8, 10.5, 18,0.5]	0.063	0.067	1524	877	37.807
[8, 10.5, 18,0.65]	0.044	0.087	1497	901	infinity
[8, 10.5, 18,0.8]	0.025	0.107	1587	917	infinity

[9, 12, 18,0.2]	0.089	0.033	1543	806	9.935
[9, 12, 18,0.35]	0.072	0.058	1482	853	16.058
[9, 12, 18,0.5]	0.056	0.083	1489	889	70.155
[9, 12, 18,0.65]	0.039	0.108	1594	911	infinity
[9, 12, 18,0.8]	0.022	0.133	1555	926	infinity
[6, 7, 21,0.2]	0.133	0.014	1567	759	7.305
[6, 7, 21,0.35]	0.108	0.025	1480	816	8.929
[6, 7, 21,0.5]	0.083	0.036	1488	859	18.762
[6, 7, 21,0.65]	0.058	0.046	1503	888	67.340
[6, 7, 21,0.8]	0.033	0.057	1490	909	infinity
[7.3, 8.8, 21,0.2]	0.110	0.016	1552	780	8.065
[7.3, 8.8, 21,0.35]	0.089	0.029	1487	834	11.618
[7.3, 8.8, 21,0.5]	0.068	0.041	1492	874	29.970
[7.3, 8.8, 21,0.65]	0.048	0.053	1486	900	infinity
[7.3, 8.8, 21,0.8]	0.027	0.066	1521	919	infinity
[8.5, 10.5, 21,0.2]	0.094	0.019	1529	799	8.768
[8.5, 10.5, 21,0.35]	0.076	0.033	1488	849	15.083
[8.5, 10.5, 21,0.5]	0.059	0.048	1510	887	63.660
[8.5, 10.5, 21,0.65]	0.041	0.062	1509	911	infinity
[8.5, 10.5, 21,0.8]	0.024	0.076	1509	928	infinity
[9.8, 12.3, 21,0.2]	0.082	0.023	1499	817	9.607
[9.8, 12.3, 21,0.35]	0.066	0.040	1490	864	21.505
[9.8, 12.3, 21,0.5]	0.051	0.057	1488	900	infinity
[9.8, 12.3, 21,0.65]	0.036	0.075	1513	922	infinity

[9.8, 12.3, 21,0.8]	0.020	0.092	1522	937	infinity
[11, 14, 21,0.2]	0.073	0.029	1552	833	14.444
[11, 14, 21,0.35]	0.059	0.050	1496	877	34.325
[11, 14, 21,0.5]	0.045	0.071	1534	912	infinity
[11, 14, 21,0.65]	0.032	0.093	1526	932	infinity
[11, 14, 21,0.8]	0.018	0.114	1591	946	infinity
[4, 6.5, 15,0.2]	0.200	0.024	1677	721	10.901
[4, 6.5, 15,0.35]	0.163	0.041	1476	780	6.173
[4, 6.5, 15,0.5]	0.125	0.059	1482	823	9.802
[4, 6.5, 15,0.65]	0.088	0.076	1527	852	18.315
[4, 6.5, 15,0.8]	0.050	0.094	1520	874	32.967
[5, 7.5, 15,0.2]	0.160	0.027	1620	741	8.386
[5, 7.5, 15,0.35]	0.130	0.047	1497	795	7.544
[5, 7.5, 15,0.5]	0.100	0.067	1534	835	13.881
[5, 7.5, 15,0.65]	0.070	0.087	1501	862	21.123
[5, 7.5, 15,0.8]	0.040	0.107	1591	882	63.796
[6, 8.5, 15,0.2]	0.133	0.031	1555	759	6.947
[6, 8.5, 15,0.35]	0.108	0.054	1493	810	8.686
[6, 8.5, 15,0.5]	0.083	0.077	1533	847	16.960
[6, 8.5, 15,0.65]	0.058	0.100	1560	871	34.483
[6, 8.5, 15,0.8]	0.033	0.123	1570	890	104.348
[7, 9.5, 15,0.2]	0.114	0.036	1564	776	8.201
[7, 9.5, 15,0.35]	0.093	0.064	1509	822	10.574
[7, 9.5, 15,0.5]	0.071	0.091	1504	857	18.856
[7, 9.5, 15,0.65]	0.050	0.118	1482	877	32.814

[7, 9.5, 15,0.8]	0.029	0.145	1543	898	466.926
[8, 10.5, 15,0.2]	0.100	0.044	1528	792	8.170
[8, 10.5, 15,0.35]	0.081	0.078	1527	834	13.320
[8, 10.5, 15,0.5]	0.063	0.111	1592	867	34.965
[8, 10.5, 15,0.65]	0.044	0.144	1550	889	87.273
[8, 10.5, 15,0.8]	0.025	0.178	1648	905	infinity
[2, 3, 12,0.2]	0.400	0.022	2061	674	infinity
[2, 3, 12,0.35]	0.325	0.039	1717	726	16.618
[2, 3, 12,0.5]	0.250	0.056	1544	766	6.996
[2, 3, 12,0.65]	0.175	0.072	1524	797	8.442
[2, 3, 12,0.8]	0.100	0.089	1507	820	10.239
[4, 5, 12,0.2]	0.200	0.029	1656	721	9.311
[4, 5, 12,0.35]	0.163	0.050	1503	763	5.898
[4, 5, 12,0.5]	0.125	0.071	1526	796	8.422
[4, 5, 12,0.65]	0.088	0.093	1520	821	10.850
[4, 5, 12,0.8]	0.050	0.114	1583	841	18.746
[6, 7, 12,0.2]	0.133	0.040	1570	759	7.401
[6, 7, 12,0.35]	0.108	0.070	1524	794	8.203
[6, 7, 12,0.5]	0.083	0.100	1564	823	13.207
[6, 7, 12,0.65]	0.058	0.130	1542	844	16.611
[6, 7, 12,0.8]	0.033	0.160	1575	861	27.350
[7, 8, 12,0.2]	0.114	0.050	1520	776	6.912
[7, 8, 12,0.35]	0.093	0.088	1509	808	8.965
[7, 8, 12,0.5]	0.071	0.125	1556	835	15.132
[7, 8, 12,0.65]	0.050	0.163	1593	855	25.765
[7, 8, 12,0.8]	0.029	0.200	1747	870	150.943

[9, 10, 12,0.2]	0.089	0.100	1542	806	9.896
[9, 10, 12,0.35]	0.072	0.175	1692	834	33.670
[9, 10, 12,0.5]	0.056	0.250	1812	857	infinity
[9, 10, 12,0.65]	0.039	0.325	1873	873	infinity
[9, 10, 12,0.8]	0.022	0.400	2083	885	infinity
[2, 3, 9,0.2]	0.400	0.033	2093	674	infinity
[2, 3, 9,0.35]	0.325	0.058	1717	716	15.715
[2, 3, 9,0.5]	0.250	0.083	1544	748	6.168
[2, 3, 9,0.65]	0.175	0.108	1580	773	8.590
[2, 3, 9,0.8]	0.100	0.133	1534	793	8.432
[3, 4, 9,0.2]	0.267	0.040	1847	699	infinity
[3, 4, 9,0.35]	0.217	0.070	1547	736	5.784
[3, 4, 9,0.5]	0.167	0.100	1566	765	7.597
[3, 4, 9,0.65]	0.117	0.130	1536	787	8.045
[3, 4, 9,0.8]	0.067	0.160	1574	805	11.178
[4, 5, 9,0.2]	0.200	0.050	1660	721	9.577
[4, 5, 9,0.35]	0.163	0.088	1507	754	5.610
[4, 5, 9,0.5]	0.125	0.125	1540	780	7.692
[4, 5, 9,0.65]	0.088	0.163	1595	801	11.826
[4, 5, 9,0.8]	0.050	0.200	1734	816	43.290
[5, 6, 9,0.2]	0.160	0.067	1559	741	6.263
[5, 6, 9,0.35]	0.130	0.117	1573	771	8.196
[5, 6, 9,0.5]	0.100	0.167	1618	795	12.559
[5, 6, 9,0.65]	0.070	0.217	1756	813	62.696
[5, 6, 9,0.8]	0.040	0.267	1762	827	86.518
[6, 7, 9,0.2]	0.133	0.100	1537	759	6.472

[6, 7, 9,0.35]	0.108	0.175	1681	787	17.848
[6, 7, 9,0.5]	0.083	0.250	1761	809	67.625
[6, 7, 9,0.65]	0.058	0.325	1852	825	infinity
[6, 7, 9,0.8]	0.033	0.400	2054	837	infinity

*Note: [6, 7, 21, 0.2] means t_1= 6 second, t_2= 7 second, t_3= 21 second and s=0.2